ISSN No:-2456-2165 https://doi.org/10.38124/ijisrt/IJISRT24MAY1201

DAYANANDA SAGAR COLLEGE OF ENGINEERING
(An Autonomous Institute affiliated to Visvesvaraya Technological University, approved by AICTE & UGC, Accredited by NAAC with 'A' grade and ISO 9001-2015 Certified Institution)

DEPARTMENT OF AERONAUTICAL ENGINEERING
(Accredited by the National Board of Accreditation, NBA)

A Project Report on

Aircraft Wing Morphing Using Auxetic Structures

(19AE8ICPR2)

Submitted in partial fulfillment for the award of the degree

BACHELOR OF ENGINEERING
in
AERONAUTICAL ENGINEERING.

Submitted By

B SHATINDRA	1DS20AE007
SAGAR V NAVALGUND	1DS20AE034
TEJAS C C	1DS20AE041
ROHITH V CHINDI	1DS21AE411

Under the guidance of,
Dr. Hareesha N.G
HOD, Department of Aeronautical Engineering
Dayananda Sagar College of Engineering
Bengaluru-560078
2023-24

ISSN No:-2456-2165 https://doi.org/10.38124/ijisrt/IJISRT24MAY1201

DAYANANDA SAGAR COLLEGE OF ENGINEERING

(An autonomous Institute affiliated to Visvesvaraya Technological University, approved by AICTE & UGC, Accredited by NAAC with 'A' grade and ISO 9001-2015 Certified Institution)

DEPARTMENT OF AERONAUTICAL ENGINEERING

(Accredited by National Board of Accreditation, NBA)

CERTIFICATE

Certified that the project work entitled **"Aircraft Wing Morphing using Auxetic Structures"** carried out by **Mr. B Shatindra (1DS20AE007), Mr. Sagar V Navalgund (1DS20AE034), Mr. Tejas C C (1DS20AE041) and Mr. Rohith V Chindi (1DS21AE411)**, and in partial fulfillment for the award of **Bachelor of Engineering** in **Aeronautical Engineering**, during the academic year 2023-24. It is certified that all corrections/suggestions indicated for internal assessment have been incorporated in the report deposited in the departmental library. The project report has been approved as it satisfies the academic requirements in respect of project work prescribed for the said degree.

Signature of the Guide	Signature of the HOD	Signature of the Principal
(Dr. Hareesha N G)	**(Dr. Hareesha N G)**	**(Dr. B. G. Prasad)**

Name of the examiners	Signature
1)	
2)	

ISSN No:-2456-2165 https://doi.org/10.38124/ijisrt/IJISRT24MAY1201

DECLARATION

We, Mr. **B Shatindra (1DS20AE007),** Mr. **Sagar V Navalgund (1DS20AE034),** Mr. **Tejas C C (1DS20AE041) and** Mr. **Rohith V Chindi** (**1DS21AE411)** hereby declare that, this dissertation work entitled **"AIRCRAFT WING MORPHING USING AUXETIC STRUCTURES"** has been carried out by us under the guidance of **Dr. Hareesha N G,** HOD, Department of Aeronautical Engineering, in partial fulfillment of the requirement of the degree **Bachelor of Engineering in Aeronautical Engineering**.

Place: Bangalore	B SHATINDRA	(1DS20AE007)
Date:		
	SAGAR V NAVALGUND	(1DS20AE034)
	TEJAS C C	(1DS20AE041)
	ROHITH V CHINDI	(1DS21AE411)

ISSN No:-2456-2165 https://doi.org/10.38124/ijisrt/IJISRT24MAY1201

ACKNOWLEDGEMENT

Before introducing our thesis work, we would like to thank the people without whom the success of this thesis would have been only a dream.

We express our deep sense of gratitude and indebtedness to **Dr. Hareesha N G**, HOD, Department of Aeronautical Engineering, for his valuable guidance, continuous assistance and in the critical appraisal of the thesis.

It is with great pleasure, we extend our gratitude and thanks to **Dr. B G Prasad**, Principal, Dayananda Sagar College of Engineering, for his encouragement throughout the project.

We feel short words to express our heartfelt thanks to all our family members and friends and all those who have directly or indirectly helped us during our course.

Place: Bangalore
Date:

B SHATINDRA (1DS20AE007)
SAGAR V NAVALGUND (1DS20AE034)
TEJAS C C (1DS20AE041)
ROHITH V CHINDI (1DS21AE411)

ISSN No:-2456-2165 https://doi.org/10.38124/ijisrt/IJISRT24MAY1201

ABSTRACT

Cellular materials exhibit two key properties: structures and mechanisms. This allows for the design of structures using cellular materials while effectively controlling both stiffness and flexibility, based on the connectivity of the struts. This study aims to explore the in-plane flexible properties of cellular materials dominated by bending under macroscopic deformation. Additionally, it seeks to establish a method for designing a passive morphing airfoil with flexible cellular cores. The investigation focuses on airfoils featuring re-entrant and S-shaped cellular cores, analyzing their behavior under static loads by examining the deformation of the cellular cores subjected to aerostatic loads. In the context of the airfoil's deformation with flexible cellular cores under aerostatic loading, shear emerges as the predominant deformation mode for the cores of the airfoil. Wings of conventional aircraft are optimized for only a few conditions, not for the entire flight envelope. Therefore, it is necessary to develop the morphing airfoil with smart structures for the next generation of excellent aircraft.

In this project, this was made possible using, re-entrant and S-shaped auxetic structures as a member of the meta-material family, with negative Poisson's ratio to enable an effortless passive morphing mechanism as it has high flexibility along in-plane direction (chord-wise). The 3D CAD Models of Re-entrant and S-shaped auxetic airframes were designed and analyzed. Initially, Static Structural analysis is performed on both airframes to observe the structure's behavior, and design modification and optimization are performed in different iterations. With a reduction in maximum equivalent stress by 20%, the Re-entrant airframe exhibits lower stress and hence more flexibility. The wings were modeled with a span of 1m using auxetic airframes, air pressure was generated using CFD analysis with MACH 0.45. Finally, the fluid-structure interaction was done by importing the air pressure and performing static structural analysis for the structural performance of wings using auxetic airframes. It was found that Re-entrant auxetic wing showed an increase of 9.99% in load carrying capacity, accompanied by a decrease of 389 grams of weight when compared to S-shaped auxetic wing.

Considering the deformation of the airframe with flexible cellular cores under a load, the re-entrant honeycomb core shows the highest flexibility in shear and causes lower stress than the S-auxetic cores. This implies that the re-entrant honeycomb core has the potential for passive morphing.

ISSN No:-2456-2165 https://doi.org/10.38124/ijisrt/IJISRT24MAY1201

TABLE OF CONTENTS

ISSN No:-2456-2165 https://doi.org/10.38124/ijisrt/IJISRT24MAY1201

LIST OF FIGURES

ISSN No:-2456-2165 https://doi.org/10.38124/ijisrt/IJISRT24MAY1201

LIST OF TABLES

ISSN No:-2456-2165 https://doi.org/10.38124/ijisrt/IJISRT24MAY1201

CHAPTER ONE
INTRODUCTION

A. Introduction

Aircraft have been a fundamental part of military power since the mid-20th century, Military aircrafts are used for combat and non-combat purposes some of them are search and rescue, reconnaissance, observation/surveillance, Early Warning, Control, transport, training, aerial refueling etc., Military aircrafts has much higher maneuverability than normal aircrafts with relaxed stability.

Relaxed stability refers to an aircraft with low or negative stability, an aircraft with negative stability will tend to change its pitch and bank angles spontaneously which can also be called as unstable aircrafts with lower stability and high speed the wing leads to various structural damage in aircraft, one of the major problem due to lower stability is flutter.

Aircraft performs various maneuvers during flight conditions and various pressure forces act around the wing. In some conditions they need to be adjusted, this action can be enabled by changing the chamber of the wing. The reduction of wing flutter in aircraft can be accomplished through various techniques, and morphing stands out as a prominent method. Traditionally, the approach involved manipulating the control surface, inducing a significant increase in curvature at the point of flow separation, resulting in excessive drag. As a result, the conventional utilization of such techniques became unlikely. However, the concept of a morphing airfoil was first proposed during the 1920s and has regained considerable attention in contemporary times.

Morphing in an aircraft wing is done to change the shape and configuration of an aircraft. It is done to improve the flight capabilities, to increase the aerodynamic performance (CL/CD ratio is always better than conventional aircraft). Moreover, with the intent of obviating the necessity of multiple control panels [1]. Morphing wing is designed to be adaptive which means to seamlessly ‘shape fit’ without any steps or slots in the wing according to the flight requirement. It increases the overall flight envelope. This is done by using “high amplitude but low frequency” technique i.e., occasionally total flight morphing is done but when it is done, it is done with much intensity. Through morphing, the drag on the aircraft is minimized, leading to an increased range, improved performance and stealth characteristics can be observed, morphing reduces the use of conventional control surfaces, it also controls flutter by “high frequency but low amplitude” which means morphing must be done more often but, in less volume, to achieve less flutter.

Morphing in aviation has given us a wide range of wing configuration options. For non-morphing aircraft, it is quite impossible to achieve different aerodynamic conditions due to an increase in cruise speed and payload leading to more rigid aircraft structures. The structural design for the wing morphing is challenging since contradicting requirements such as flexibility, load-carrying capacity, and lightweight need to be satisfied

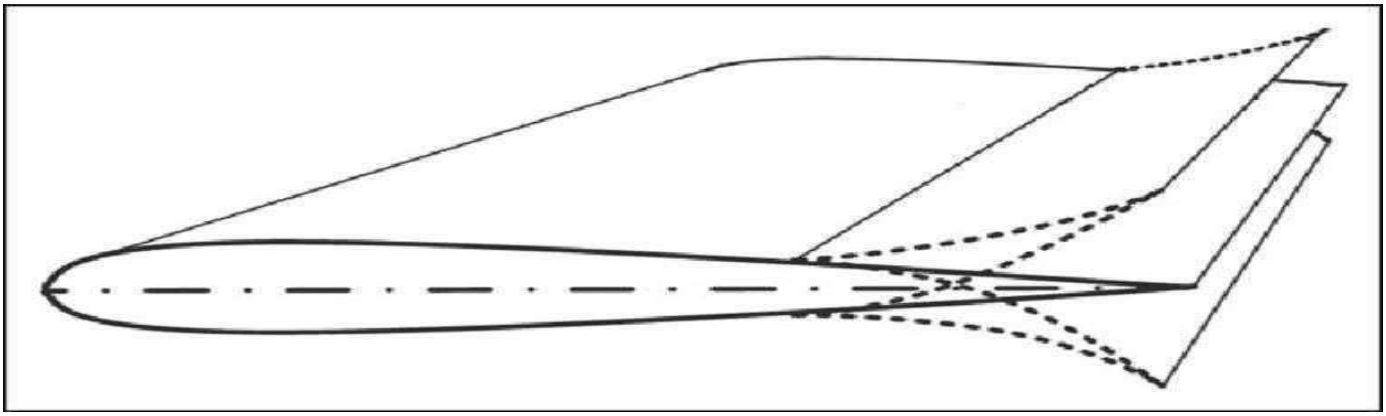

Fig 1: Chord-Wise Morphing of an Aircraft Wing

Finding a lightweight, compact, energy-efficient, and foolproof morphing actuator poses yet another hurdle. One potential solution lies in the utilization of a smart material actuator capable of directly transforming electrical, magnetic, or thermal stimuli into mechanical displacement. This approach holds promise in meeting certain prerequisites [2]. Metamaterials are unique materials having unusual physical properties with negative or extreme values than usual materials, meta means ‘‘Superior’’ they can be categorized according to their characteristic changes, few main classes are – elastic metamaterials, mechanical metamaterials, and truss metamaterials. One such metamaterial having a negative Poisson’s ratio which exhibits a counter-intuitive behavior are called auxetic materials. Honeycomb structures are natural or man-made structures that have the geometry of honeycombs to allow the minimization of the amount of used material to reach minimal weight and minimal material cost. Types of honeycomb structures are dependent upon the geometrical shape.

ISSN No:-2456-2165 https://doi.org/10.38124/ijisrt/IJISRT24MAY1201

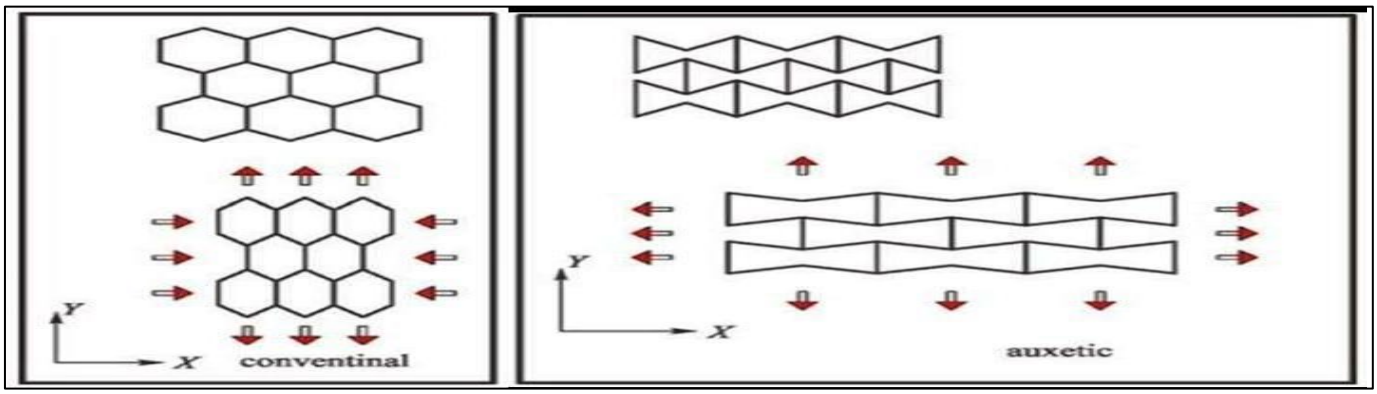

Fig 2: Honeycomb Structures

Honeycomb structures are natural or man-made structures that have the geometry of a honeycombs to allow the minimization of the amount of material used to reach minimal weight and minimal material cost. Types of honeycomb structures are dependent upon the geometrical shape.

B. Outline of Thesis

- **CHAPTER 1:** This chapter provides a brief introduction about aircraft, the advantages of morphing, and detailed characteristics of auxetic structures.
- **CHAPTER 2:** This chapter consists of the different literature surveys that we have studied to help and guide us with our project work.
- **CHAPTER 3:** This chapter provides details regarding our project's objectives, the problem statement of the work, and the methodology flow of our project.
- **CHAPTER 4:** This chapter provides detailed modelling and description of the airfoils and the deformation and stresses acting on them.
- **CHAPTER 5:** Modelling of auxetic wings to study the air-pressure loads acting on the upper and lower surface of the auxetic wings through fluid dynamic analysis.
- **CHAPTER 6:** This chapter provides the overall conclusion of our project and its results

ISSN No:-2456-2165 https://doi.org/10.38124/ijisrt/IJISRT24MAY1201

CHAPTER TWO
LITERATURE REVIEW

A. Introduction

The literature review looks into the journals and textbooks referred for this project. They formed the foundation of the project and provided invaluable data on how to proceed and take the suitable steps in completing the project.

B. Literature Review

Sivambika et.al., [1] emphasize the concept of using auxetic structures for passive morphing to control flutter. It was found that incorporating an auxetic structure resulted in weight reduction and delay in flutter, thereby increasing the flight performance characteristics. FSI analysis was carried out on wings to find the aerodynamic behavior. Finally, modal and harmonic analysis was performed and it was seen that auxetic wings performed better compared to regular Eppler wings.

P R Budarapu et.al., [2] This paper is categorized into two parts. (1) A framework to design the aircraft wing structure and (2) analysis of a morphing airfoil with auxetic structure. The properties of auxetic structures for elliptical and circular nodes are investigated. The innovative configuration of the auxetic framework seamlessly integrates into the airfoil contour, delivering exceptional flexural adaptability along its chord-wise axis, alongside remarkable torsional load-bearing capabilities. The study concludes that the developed strength-based design framework effectively determines the component sizes for a composite aircraft wing structure under aerodynamic loading conditions, with the numerical model demonstrating acceptable natural frequencies under extreme loads. The compliance characteristics of the auxetic airfoil, validated through numerical modeling, align closely with experimental results, confirming the efficacy of the design approach for both the wing structure and the morphing airfoil.

Hyeonu Heo et.al., [3] focus on the utilization of compliant cellular structures to achieve passive morphing capabilities in airfoil designs. The findings demonstrate the potential of compliant cellular structures to autonomously alter their shape in response to aerodynamic forces, leading to improved performance across different flight conditions. The study concludes that the re-entrant hexagonal honeycomb core demonstrates the highest flexibility in shear and induces lower stress in local cell walls compared to chiral and regular hexagonal honeycomb cores when designed to have the same shear modulus. This superior flexibility and reduced local stress make the re-entrant hexagonal honeycomb core a promising candidate for use in passive morphing applications.

Paolo Bettini et.al., [4] investigates the application of composite chiral structures in the development of morphing airfoils, focusing on both numerical analyses and the advancement of a tailored manufacturing process. Through a combination of computational simulations and experimental validation, the mechanical properties and aerodynamic performance of these structures are thoroughly examined. The study concludes that composite cellular structures with a chiral topology offer significant advantages in terms of large displacement capabilities with minimal component straining, making them suitable for morphing airfoil designs. The numerical analysis demonstrates that composite materials outperform metallic structures in this context. Detailed numerical models confirm the strength and viability of these composite configurations, highlighting their potential for advanced aerospace applications, particularly in designing efficient and flexible morphing airfoils.

A Alderson et.al., [5] have studied the developments in the modelling, design, manufacturing, testing, and potential applications of auxetic cellular solid and polymers among others. Auxetic composite laminates and composites containing auxetic constituents were reviewed and enhancements in fracture toughness, velocity impact performance to demonstrate potential in energy absorbent components. The review concludes that auxetic materials offer significant potential across various aerospace engineering applications due to their unique mechanical properties, such as negative Poisson's ratio. Auxetic cellular solids, especially in honeycomb and foam forms, show promise in diverse applications from structural components to energy absorption and adaptive systems. Additionally, the potential of auxetics in sensor and actuator technologies, including strain amplification and structural health monitoring, further underscores their versatility and transformative potential in aerospace engineering.

Avinash Mohan et.al., [6] focused on the impact behavior of S-shaped and re-entrant auxetic structures fabricated using FDM. The drop mass impact tests were conducted on the auxetic structures. FEA was also undertaken to simulate and validate the impact behavior with experimental results. The study concludes that S-shaped auxetic structures fabricated using Fused Deposition Modeling (FDM) demonstrate superior compressive plateau stress and energy absorption capacity compared to re-entrant auxetic structures. This finding underscores the potential of S-shaped auxetic structures for high-impact applications in aerospace, automotive, and biomedical sectors. The deformation modes and failure mechanisms identified through FEA provide valuable insights into optimizing auxetic structures for enhanced performance in crashworthy applications.

Kusum Meena et.al., [7] have evaluated the stress concentration aspects of a standard re-entrant auxetic structure. A new structure was designed and proven to be less stressed in comparison with the re-entrant form commonly reported in their literature. Analytical, experimental, and numerical results confirm that the new structure not only improves stress distribution but also enhances auxetic behavior, sustaining a negative Poisson's ratio up to -2.5 and performing effectively under external strains up to 15%. These

ISSN No:-2456-2165 https://doi.org/10.38124/ijisrt/IJISRT24MAY1201

findings suggest that the new structure is more robust and potentially more effective for applications requiring high auxetic performance, thereby advancing the understanding and application of auxetic materials in engineering designs.

Zeyao Chen et.al., [8] Combined with the actuators, sensors, and controller techniques, the smart airfoil will bring a revolution for aircraft. Hence, the design of a smart structure that applies to the morphing airfoil is the first step, especially the flexible airfoil which exhibits many more changeable degrees than rigid structures. In this paper, the composite structure based on re-entrant quadrangular is designed to be applied in deformable aircraft. The study concludes that morphing airfoils incorporating re-entrant quadrangular auxetic lattice structures offer significant benefits, including high deformability, ease of control, variable stiffness, and the ability to withstand large stresses. The enhanced re-entrant lattice structure shows superior stiffness compared to the original design, without compromising flexibility. The FEM analysis confirms that the morphing airfoil meets the necessary mechanical performance criteria, including natural modal frequencies within acceptable limits.

Krishna Prasath Logakannan et.al., [9] In this study, the mechanical performance of a three-dimensional (3D) re-entrant structure subjected to dynamic compression was experimentally investigated using a high-speed Instron machine. A finite element (FE) model was developed using ABAQUS/Explicit and validated against the dynamic test results in terms of deformation mode, plateau stress, and Poisson's ratio. The validated FE model was subsequently employed to study the effects of the number of unit cells, geometrical parameters (aspect ratio, H/L, and re-entrant angle, θ) of the re-entrant unit cell, and compressive velocity. The results showed that the structure with $H/L = 1$ and $\theta = 45°$ had the highest specific energy absorption (SEA) when compressed in the Z direction and the structure with $H/L = 1.1$ and $\theta = 75°$ had the highest SEA when compressed in the X direction.

ISSN No:-2456-2165 https://doi.org/10.38124/ijisrt/IJISRT24MAY1201

CHAPTER THREE
OBJECTIVES AND METHODOLOGY

A. Objectives

- To model an Eppler-420 airfoil with Re-Entrant Auxetic Structure and validate it with reference paper.
- To model an Eppler-420 airfoil that incorporates a S-shaped auxetic pattern.
- Performing Static Structural Analysis of both airfoils with auxetic structures to check the flexibility of the auxetic structure.
- Modelling of wings using the above 2 auxetic airfoil ribs.
- Performing CFD analysis of wing to obtain air-loads acting on the wing and importing the loads on wings for structural analysis of wings.
- Performing structural analysis on both wings to check the structural performance of the wings. Comparing the results obtained.

B. Problem Statement

In the aviation domain, the aerodynamic and structural aspects of flight operations have consistently exerted a notable influence on performance as well as concerns related to flutter, fatigue failure, and structural integrity such as cracks. Traditional approaches like wing morphing have been explored to address flutter issues, but these methods are intricate and often come with substantial costs. In our project, we have chosen to employ auxetic structures, a straightforward and compliant mechanism for wing camber morphing.

C. Methodology

- Modelling of Eppler-420 airfoil with auxetic structure using SOLIDWORKS resulting in Re-entrant and S-shaped auxetic frame.
- Conducting static structural analysis on the two airfoils using ANSYS and comparing the results and plotting respective graphs.
- Performing CFD analysis on wings to obtain air-loads on the wings and the respective pressure contour.
- Conducting static structural analysis on both auxetic wing structures by importing air-loads and comparing the results.

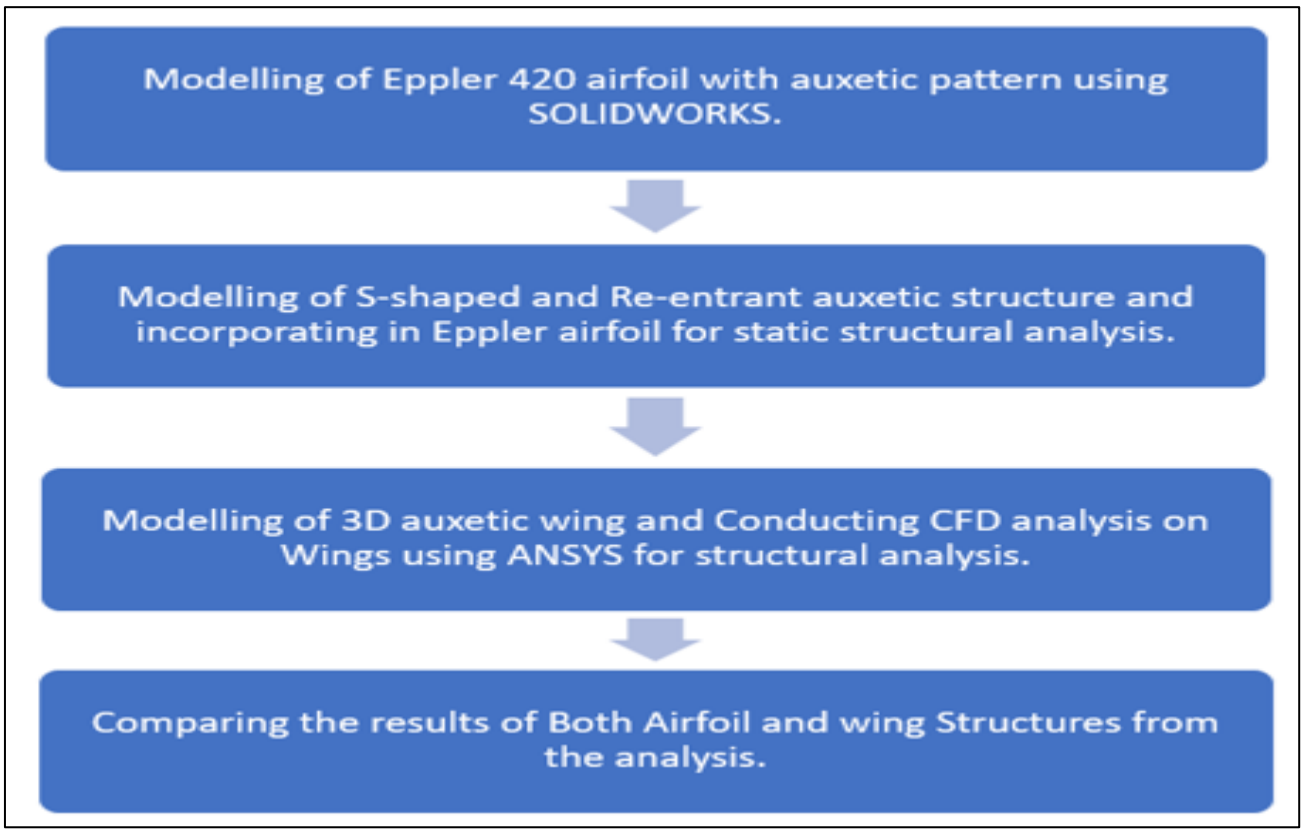

Fig 3: Flow Chart for Methodology

ISSN No:-2456-2165 https://doi.org/10.38124/ijisrt/IJISRT24MAY1201

CHAPTER FOUR
STRUCTURE MODELLING

A. Eppler-420 Airfoil

The Eppler-420 airfoil is chosen to perform the experimentation, as mentioned its high camber configuration is ideal to capture the large de-cambering deformation effects, achieved by employing an auxetic core. An S-shaped auxetic structure was used for our work. As suggested in [6] the auxetic structure which can be seen in Figure 4 (b) was taken as a reference. There are also many auxetic patterns like chiral structures, re-entrant, honeycomb, etc. However, the main focus is on S-shaped auxetic structure for our project. Having taken as a reference from [3], below parameters from Table 4.1 were used for airfoil modelling.

Table 1: Design Parameters

Symbol	Parameters	Dimension (mm)
t	Thickness	2.53
a	Distance from Leading Edge	110
b	Distance from Trailing Edge	235
c	Chord Length	700

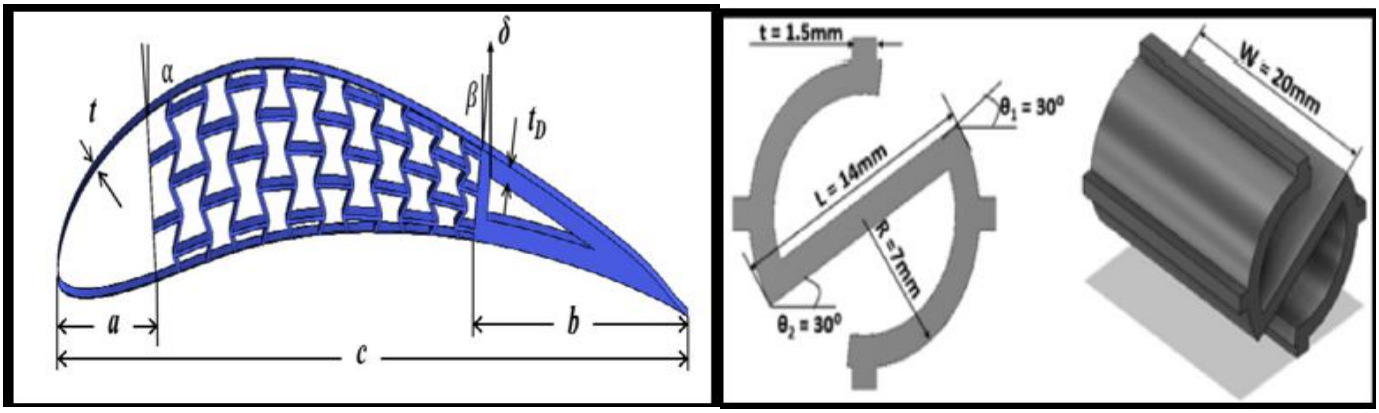

(a) (b)

Fig 4: Reference Sketch of Auxetic Airframe

Geometric mapping of the auxetic structure used is shown in Figure 4 (a). The re-entrant honeycomb core and S-auxetic core of the airfoil and rigid support at the trailing edge were designed in SOLIDWORKS. The parts in the 3D view are shown in Figures 5 and 6 and Figures 7 and 8 respectively. The auxetic core was fitted into the airframe through geometric mapping in SOLIDWORKS and then the assembly was completed using ANSYS Space claim 2023. The assembly of the airframes with the auxetic core is shown in Figures 9 and 10 respectively.

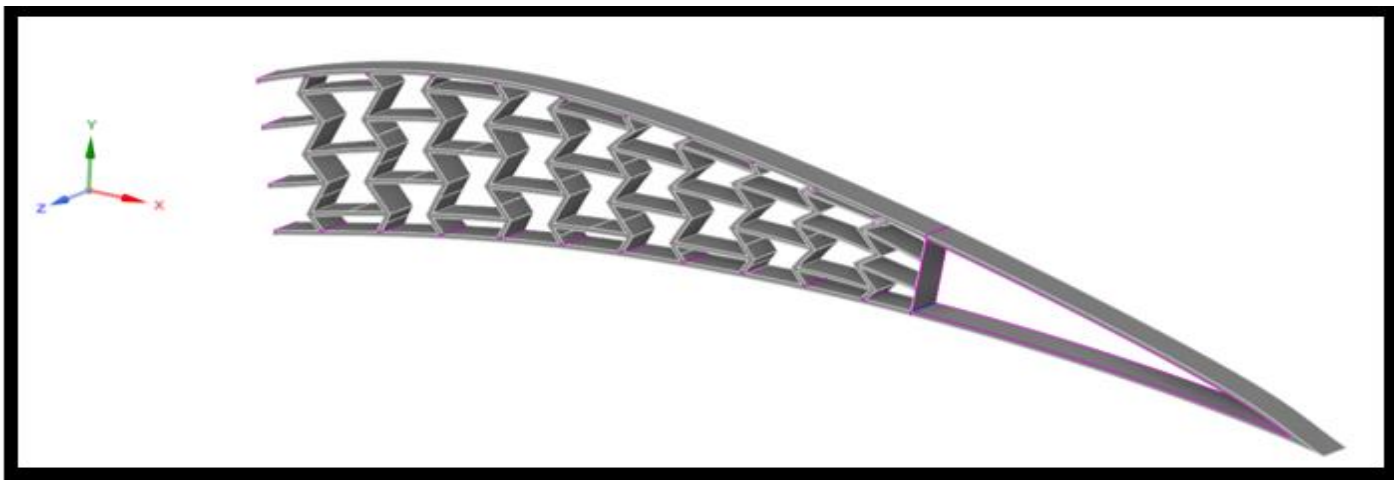

Fig 5: Re-Entrant Honeycomb Core

ISSN No:-2456-2165 https://doi.org/10.38124/ijisrt/IJISRT24MAY1201

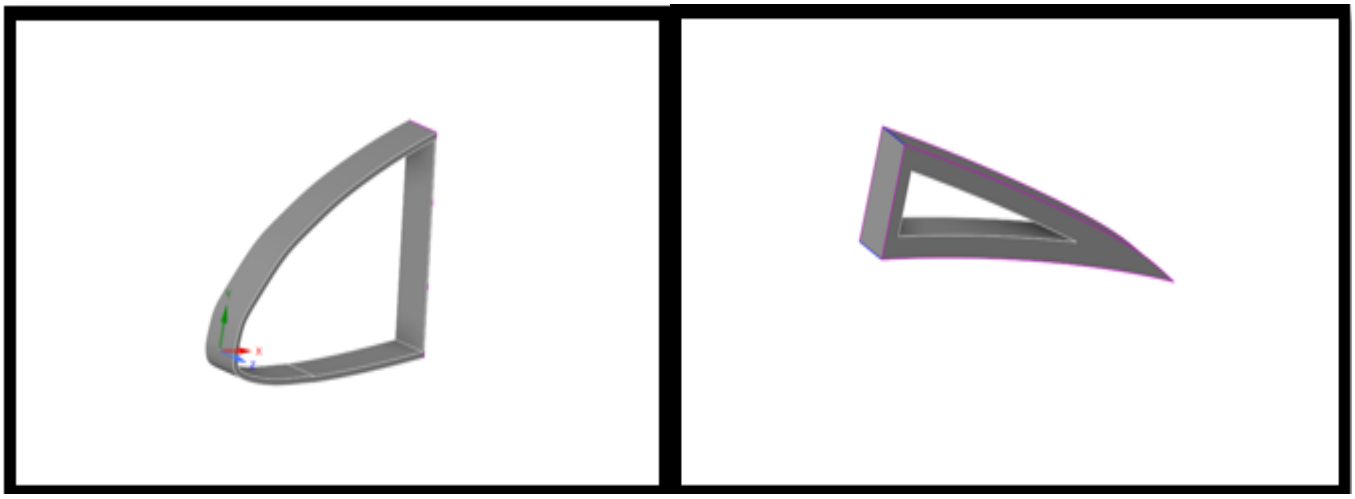

(a) (b)

Fig 6: Leading Edge and Trailing Edge of Re-Entrant Airframe

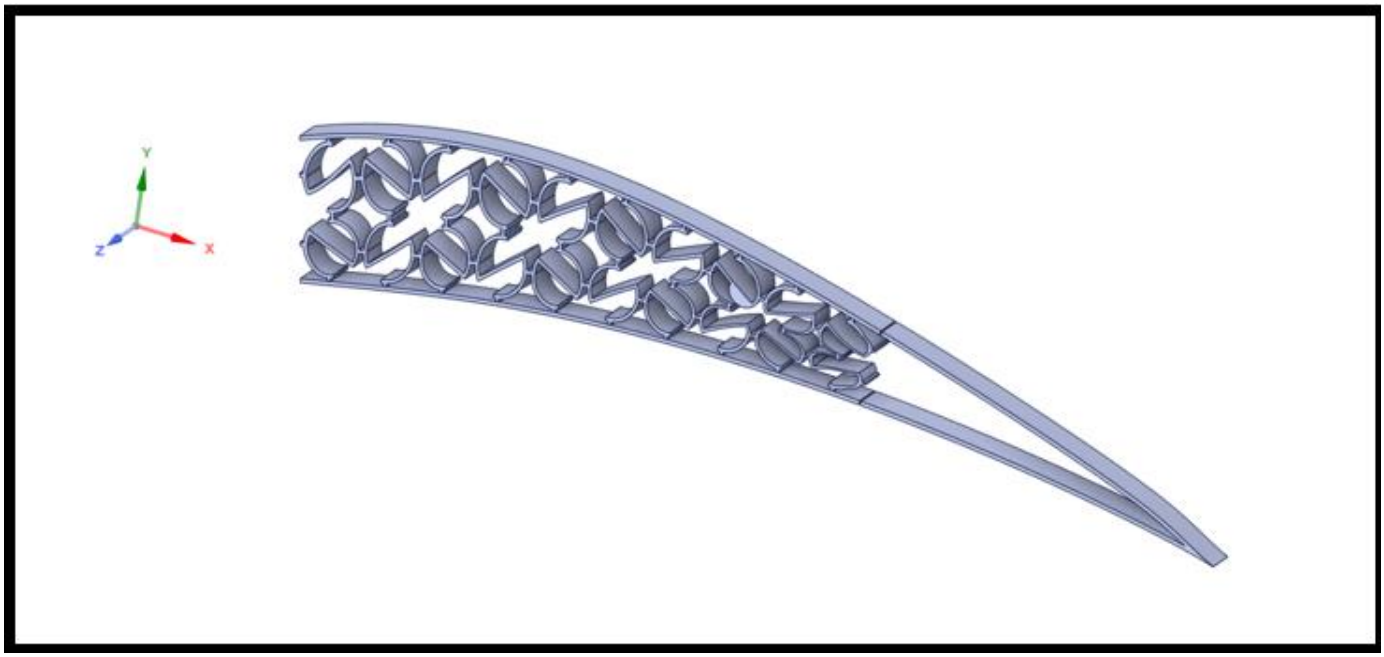

Fig 7: S-Auxetic Core

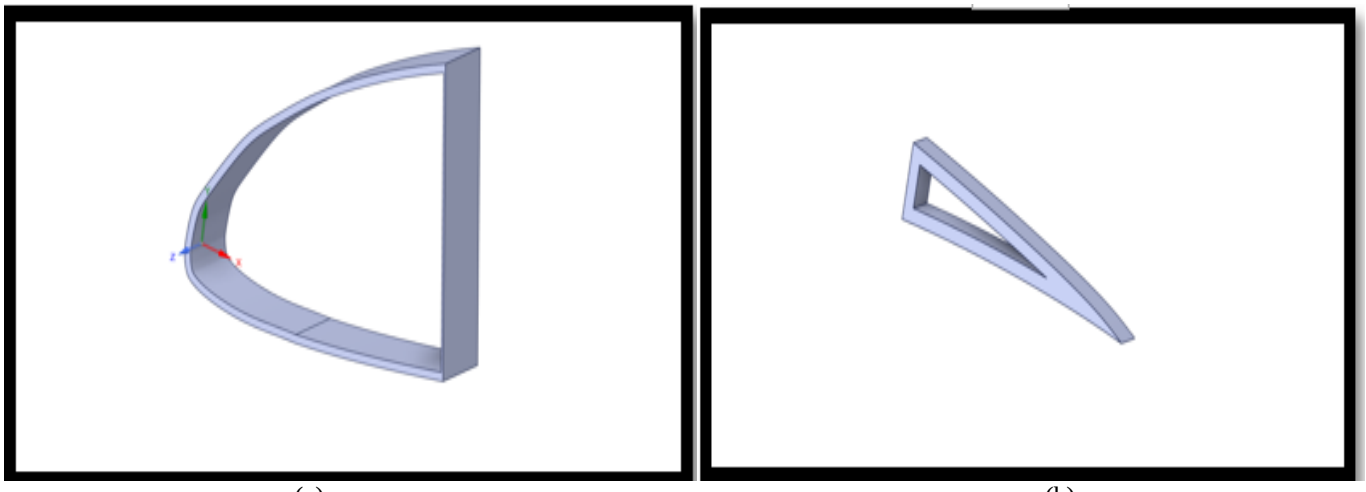

(a) (b)

Fig 8: Leading Edge and Trailing Edge of S-Auxetic Airframe

ISSN No:-2456-2165 https://doi.org/10.38124/ijisrt/IJISRT24MAY1201

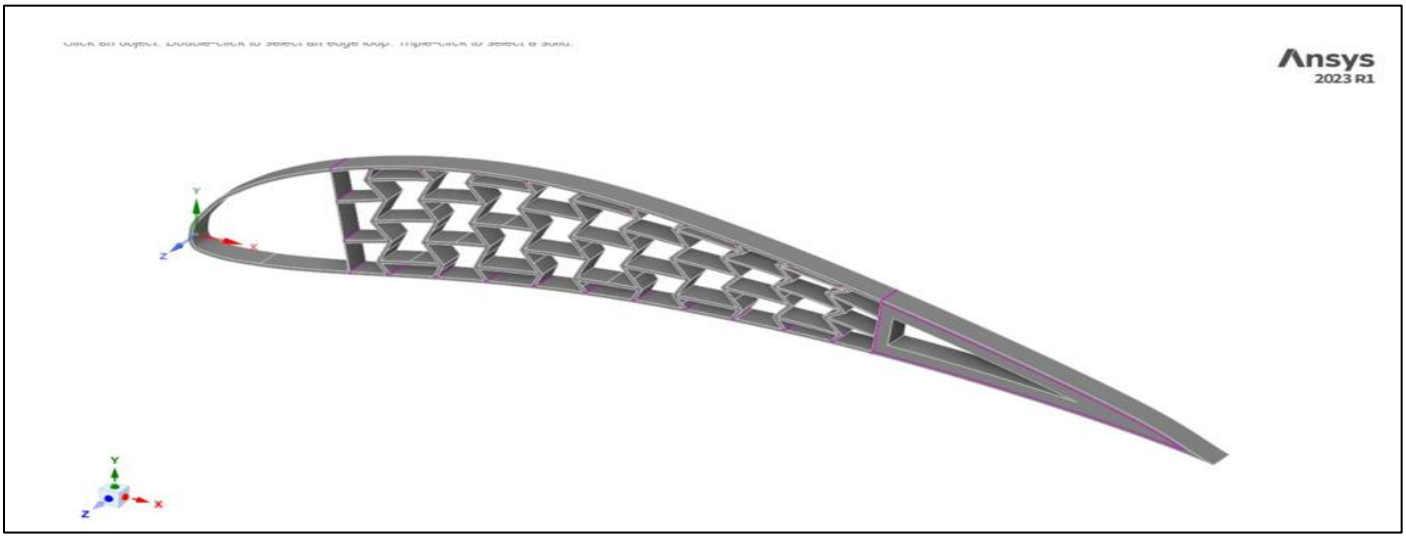

Fig 9: 3D Model of Re-Entrant Auxetic Airframe

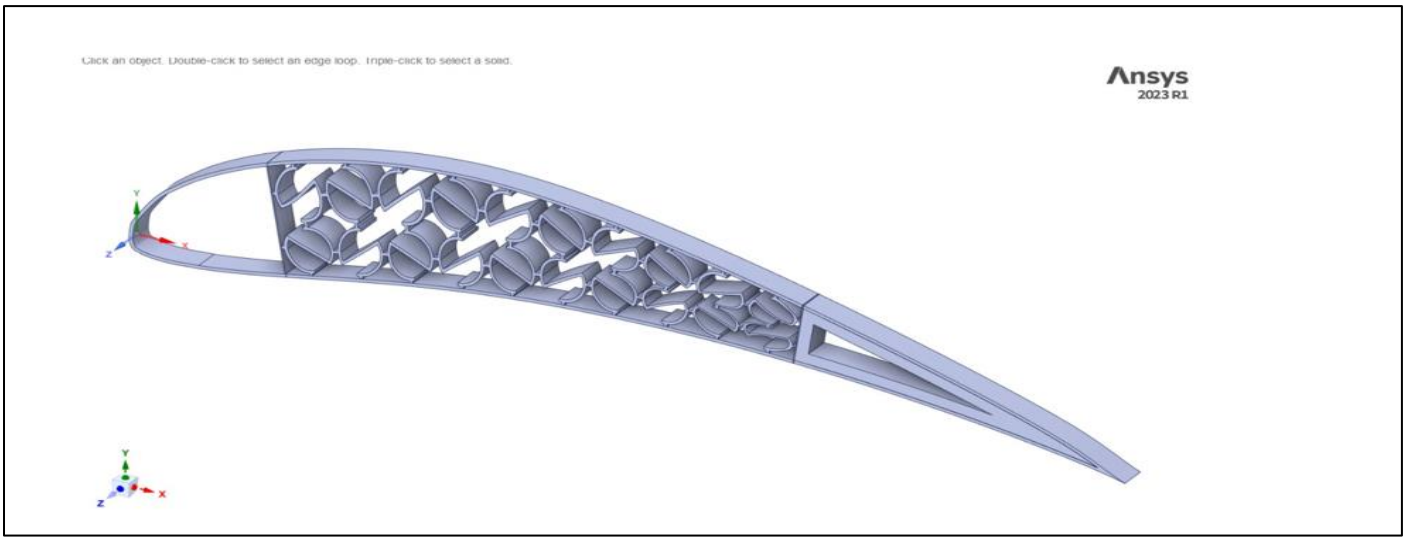

Fig 10: 3D Model of S-Shaped Auxetic Airframe

The final models of both Re-entrant and S-shaped Auxetic Structures are shown above in Figure 4.6 and Figure 4.7 respectively.

B. Meshing of Auxetic Airfoil RIB

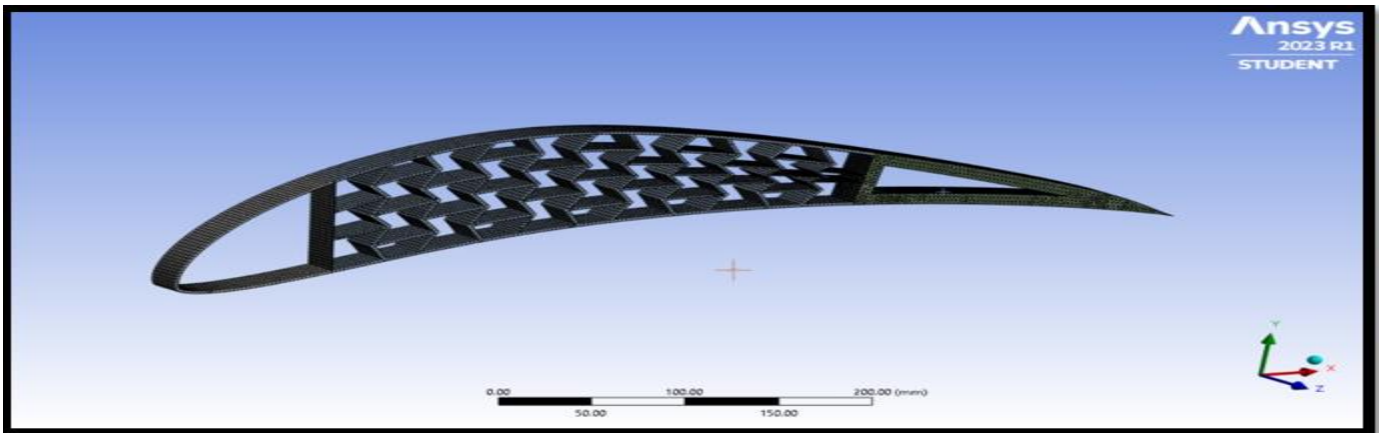

Fig 11: Meshing of Re-Entrant Auxetic Structure

ISSN No:-2456-2165 https://doi.org/10.38124/ijisrt/IJISRT24MAY1201

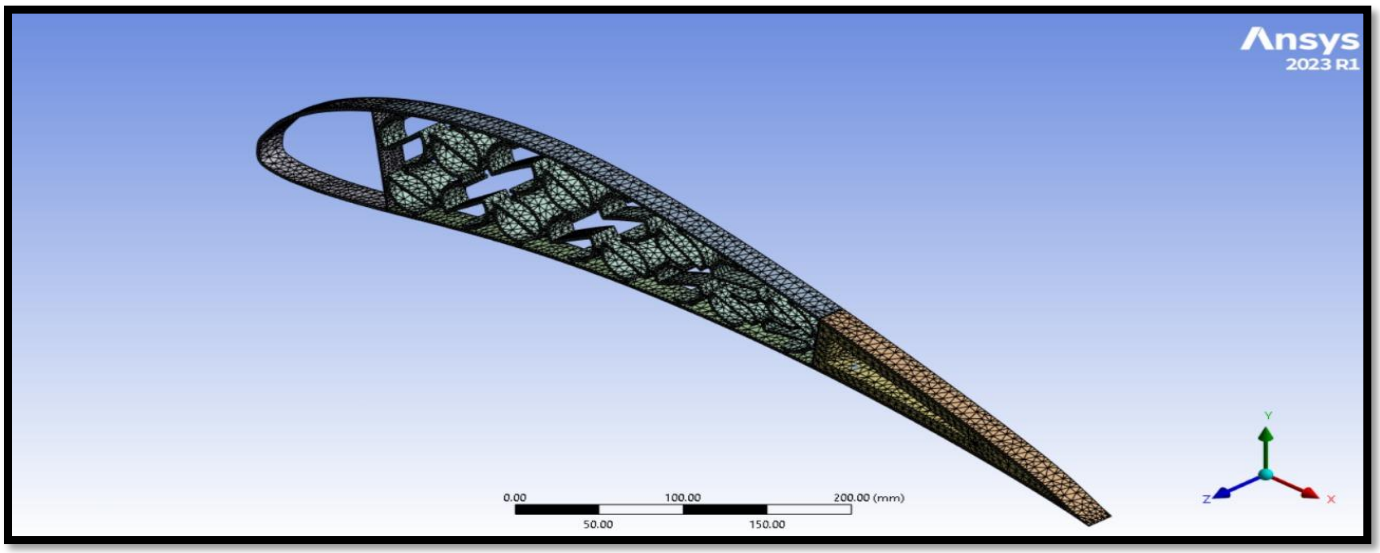

Fig 12: Meshing of S-Shaped Auxetic Structure

With an element size of 10mm, linear and tetrahedral elements were utilized while designing these structures, and the meshing of these structures is shown above in Figure 7 and Figure 8. Then static structural analysis was performed on the airframe to yield further results through ANSYS.

C. Static Structural Analysis

The static structural analysis is started with the material assignment. Aluminium 6061- T651 is used for both airframes of the auxetic core. The material properties are inputted as per the reference [1] is shown in Table 2. The geometry is meshed using tetrahedral elements because they produce good quality of mesh as per the reference [4]. Through grind independence study, the optimum element size was found to be 10mm and the meshed view of airfoil with auxetic cores is shown in Figure 11 and Figure 12.

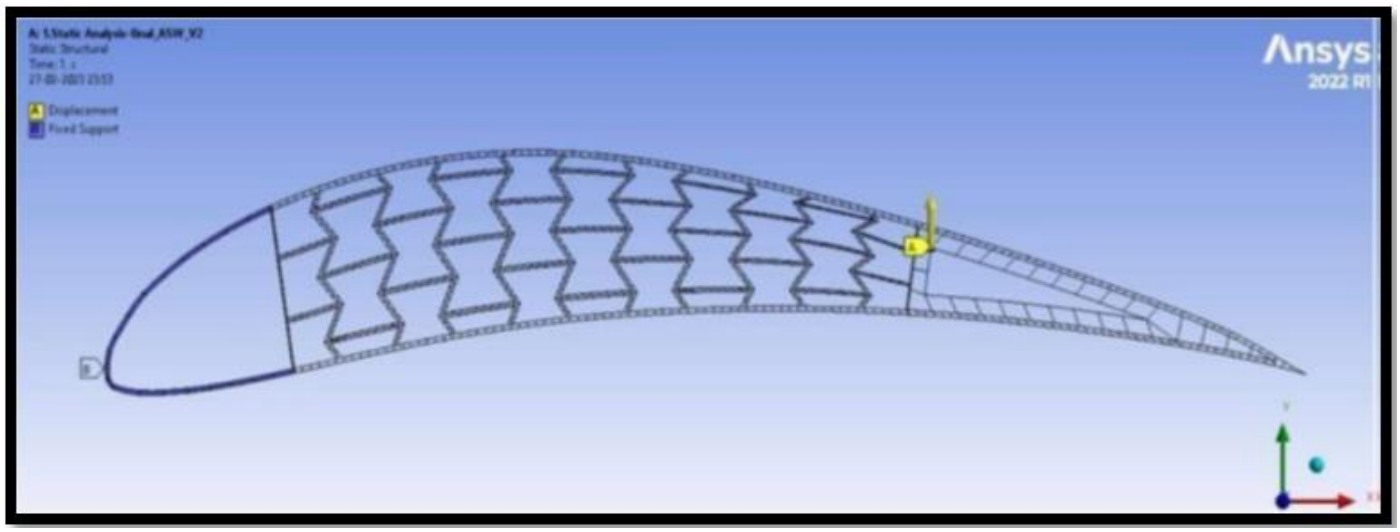

Fig 13: Boundary Conditions as Per Base Paper

The leading edge is fixed, and the load is applied at the upper vertex of the trailing edge. The trailing edge displacement along the Y-axis is computed by probing. The resultant graph obtained by conducting a static structural analysis is shown for each trial. The deformation and stress on these structures were initially calculated with a load of 50N, as per the reference [3]. It is increased in terms of 50N with every trial up to 300N. Thus, obtaining the resultant directional deformation and equivalent stress of the structure due to the applied boundary conditions for subsequent trials. Here, structural optimization is done to obtain the desired results by improving the auxetic design. After the results are noted and studied, they're compared to each other by plotting, Load (N) vs Trailing edge deflection (mm) and Load (N) vs Equivalent stress (MPa) graph from both structures. Aluminium 6061-T6 having an ultimate tensile strength of 310MPa was assigned as the material as per the reference [1]. The properties of the material can be seen in Table 2.

ISSN No:-2456-2165 https://doi.org/10.38124/ijisrt/IJISRT24MAY1201

Table 2: Material Properties

Aluminium-6061 Parameter	Value
Density	2700Kg/m³
Young's Modulus	68900 MPa
Poisson Ratio	0.33
Bulk Modulus	67549 MPa
Shear Modulus	25902 MPa
Tensile Yield Strength	276 MPa
Tensile Ultimate Strength	310 MPa

➢ *Re-Entrant Structure*

The static structural analysis starts with the material assignment, where the leading edge is fixed and the load is applied at the upper vortex of the trailing edge as shown in Figure 14. The load is applied at the upper vortex edge of the trailing edge to understand the flexibility and the deformation and the bending moments of the trailing edge of the airframe.

Directional deformation and stresses on the structures were calculated using load methods where initially 50N is applied to check the structure's behavior and increase with a factor of 50 to 300N.

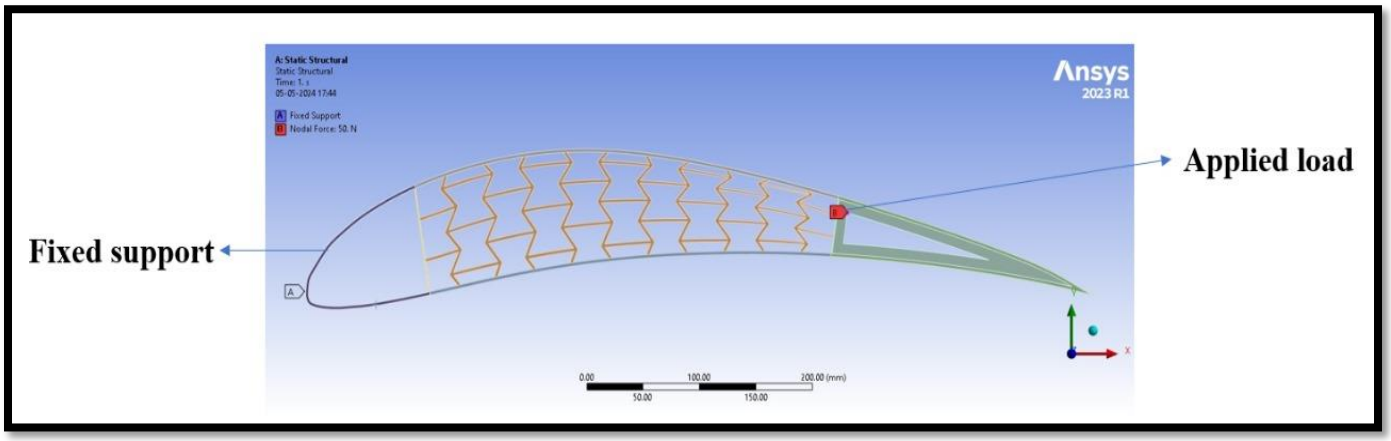

Fig 14: Boundary Conditions

- ***Trial 1****: Load Applied – 50N*

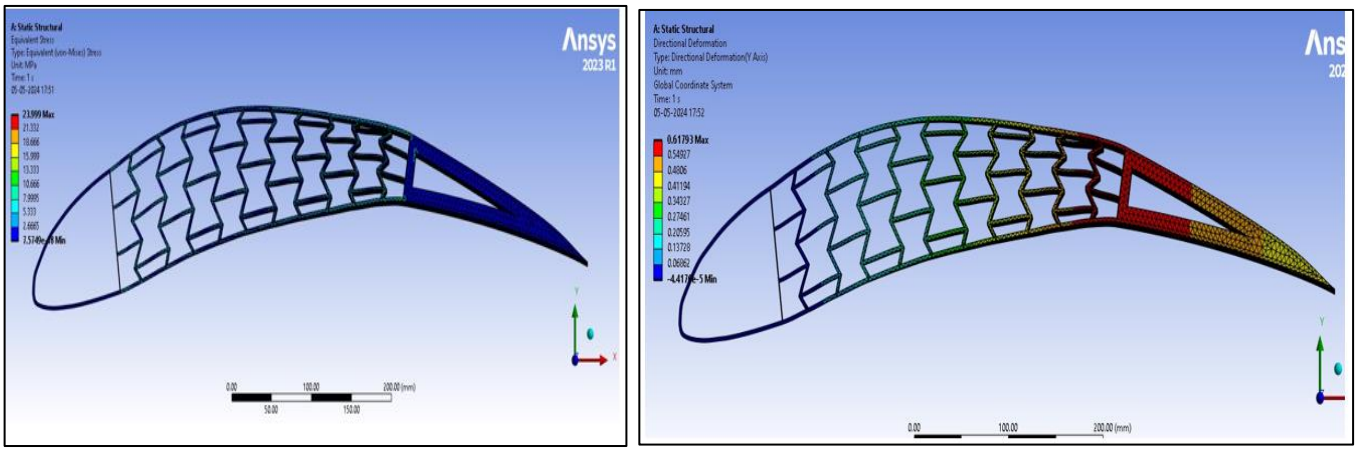

(a) (b)

Fig 15: Maximum Deflection and Maximum Stress for 50N Load Applied

For the load of 50N, the maximum stress and maximum deflection of the Re-entrant auxetic airframe is 23.399 MPa and 0.618mm as shown in Fig 15 (a) and (b) respectively.

ISSN No:-2456-2165 https://doi.org/10.38124/ijisrt/IJISRT24MAY1201

- ***Trial 2****: Load Applied – 100N*

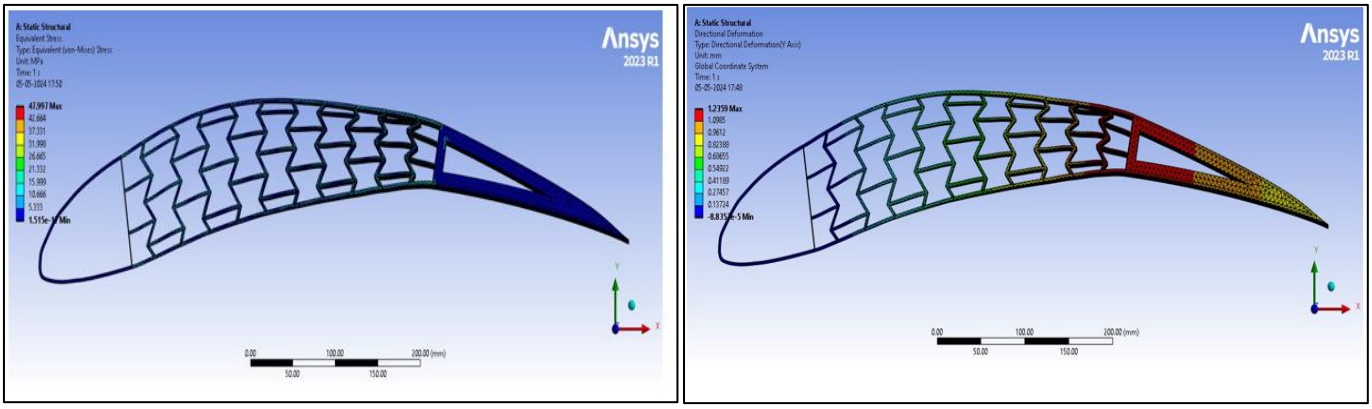

(a) (b)

Fig 16: Maximum Stress and Maximum Deflection for 100N Applied

For the load of 100N, the maximum stress and maximum deflection of the Re-entrant auxetic airframe is 47.99 MPa and 1.236mm as shown in Fig 1613 (a) and (b) respectively.

Trial 3: Load applied – 200N

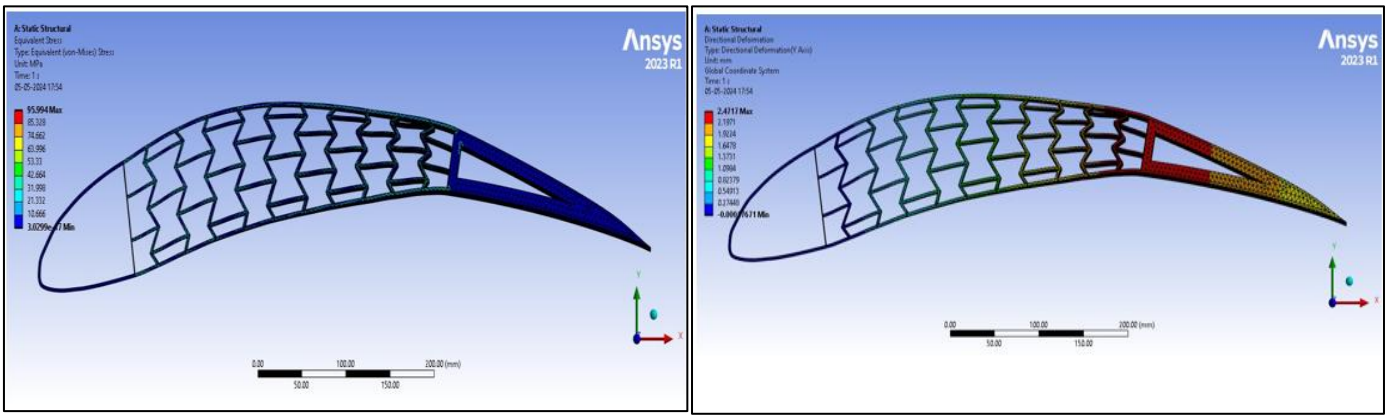

(a) (b)

Fig 17: Maximum Stress and Maximum Deflection for 200N Applied.

For the load of 200N, the maximum stress and maximum deflection of the Re-entrant auxetic airframe is 95.994 MPa and 2.471mm as shown in Fig 17 (a) and (b) respectively.

- ***Trial 4:*** *Load Applied – 300N*

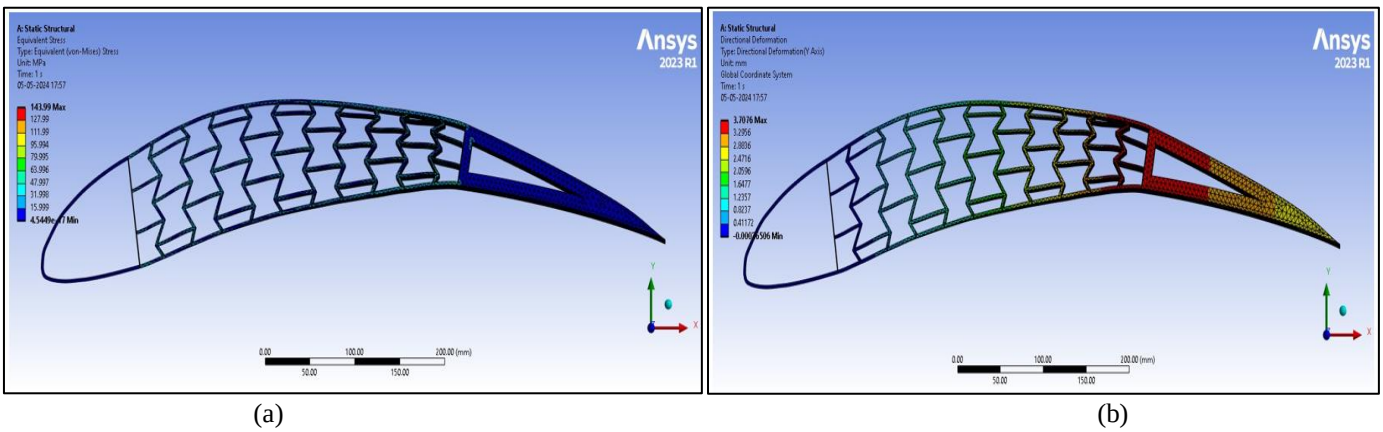

(a) (b)

Fig 18: Maximum Stress and Maximum Deflection for 300N Applied

ISSN No:-2456-2165 https://doi.org/10.38124/ijisrt/IJISRT24MAY1201

For the load of 300N, the maximum stress of the Re-entrant auxetic-structured airframe is 143.99 MPa and 3.71mm as shown in Fig 18 (a) and (b) respectively.

Similarly, the same analysis is performed for the S-auxetic airframe as shown in section 4.3.2.

The results can be authenticated by a grid independence study for the structural mesh of the re-entrant airframe for the applied load of 300N. The plot between different element sizes and total deformation shows convergence at a value of 3.71mm as shown in Figure 19.

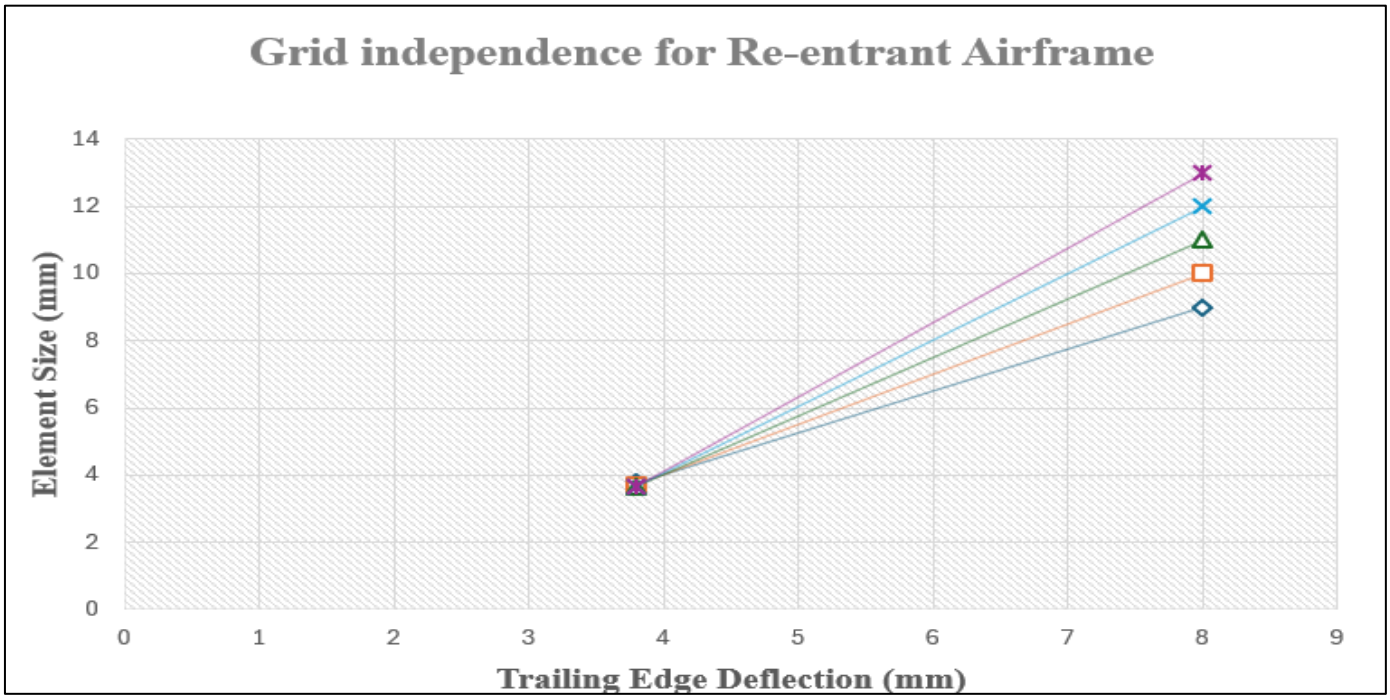

Fig 19: Grid Independence Chart for Re-Entrant Airframe

➢ *S-Auxetic Structure*

- ***Trial 1:*** *Load Applied – 50 N*

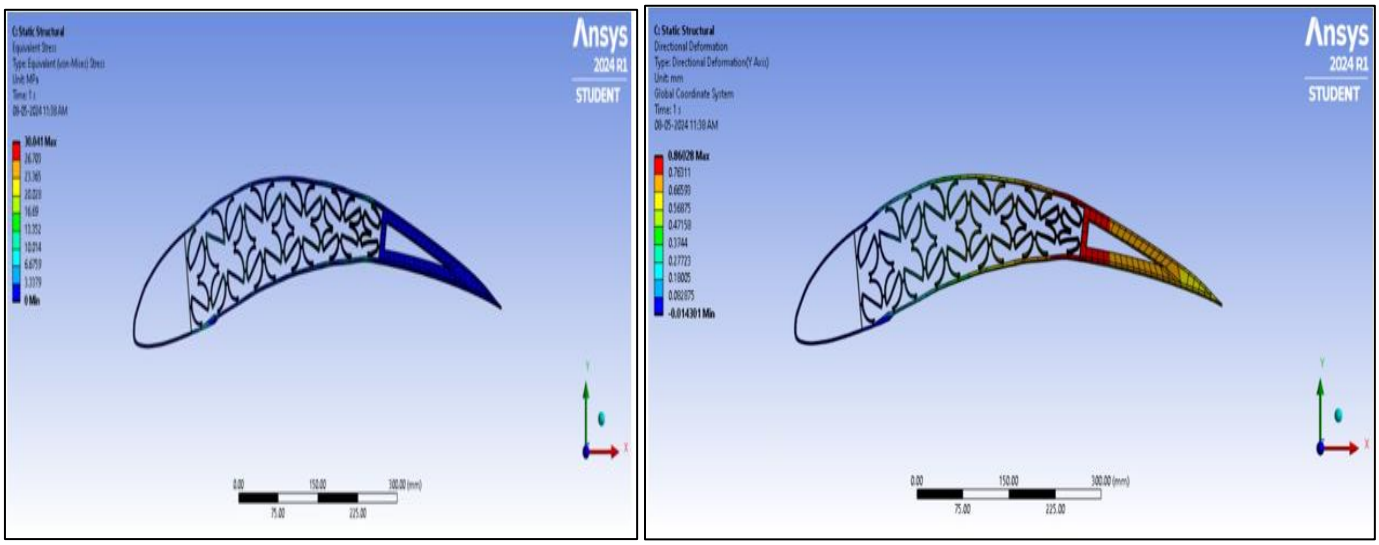

(a) (b)

Fig 20: Maximum Stress and Maximum Deflection for 50N Applied

For the load of 50N, the maximum stress and maximum deflection of the S-shaped auxetic airframe is 30.041 MPa and 0.8602mm as shown in Fig 20 (a) and (b) respectively.

ISSN No:-2456-2165 https://doi.org/10.38124/ijisrt/IJISRT24MAY1201

- ***Trial 2:*** *Load Applied – 100 N*

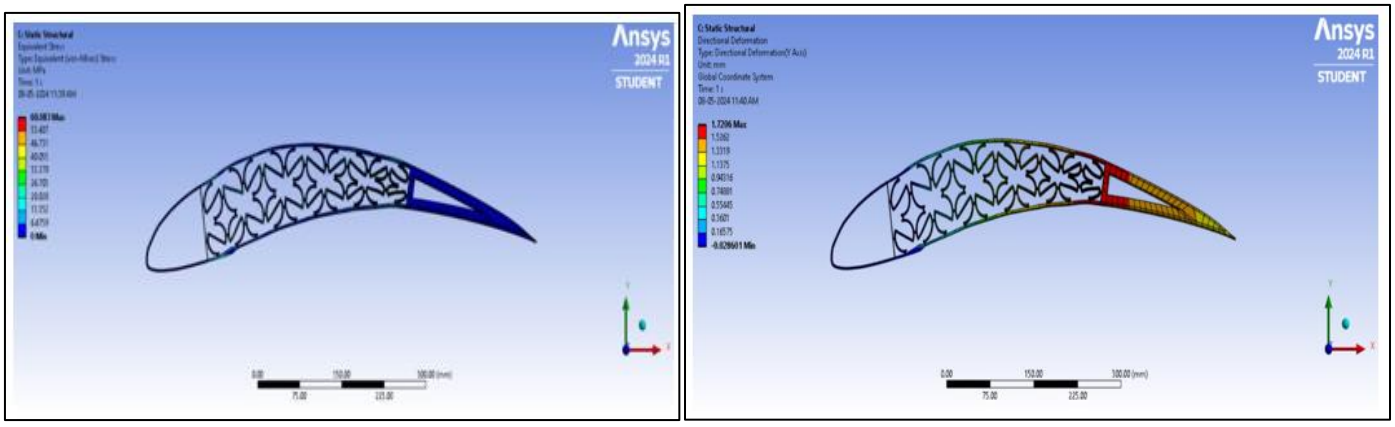

(a) (b)

Fig 21: Maximum Stress and Maximum Deflection for 100N Applied

For the load of 100N, the maximum stress and maximum deflection of the S-shaped auxetic airframe is 60.083 MPa and 1.7206mm as shown in Fig 21 (a) and (b) respectively.

- ***Trial 3:*** *Load Applied – 200 N*

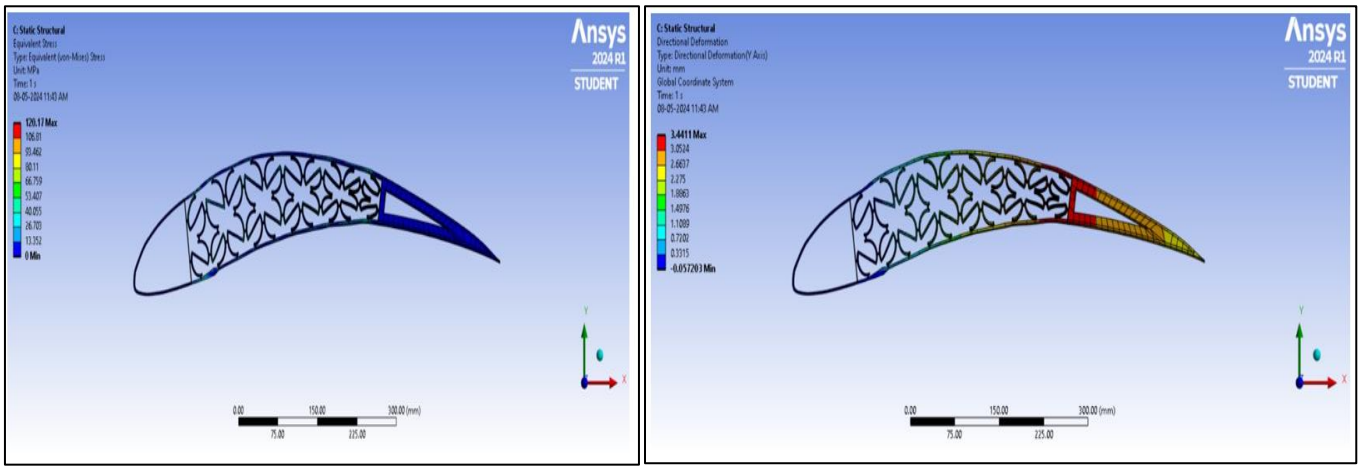

(a) (b)

Fig 22: Maximum stress and maximum deflection for 200N applied.

For the load of 200N, the maximum stress and maximum deflection of the S-shaped auxetic airframe is 120.17 MPa and 3.441mm as shown in Fig 22 (a) and (b) respectively.

- ***Trial 4:*** *Load applied – 300 N*

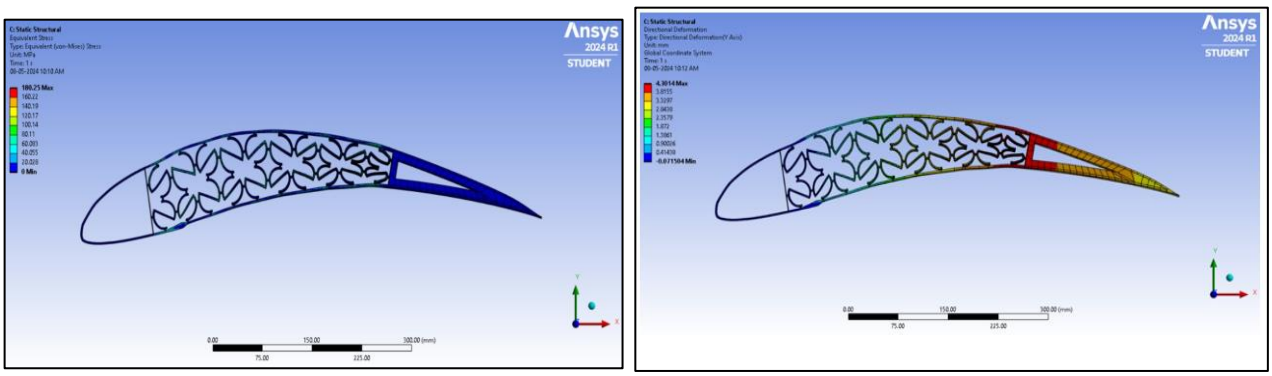

(a) (b)

Fig 23: Maximum Stress and Maximum Deflection for 300N Applied

ISSN No:-2456-2165 https://doi.org/10.38124/ijisrt/IJISRT24MAY1201

For the load of 300N, the maximum stress and maximum deflection of the S-shaped auxetic airframe is 180.25 MPa and 5.17mm as shown in Fig 23 (a) and (b) respectively.

The results can be authenticated by a grid independence study for the structural mesh of the S-auxetic airframe for the applied load of 300N. The plot between different element sizes and total deformation shows convergence at a value of 5.17mm as shown in Figure 24.

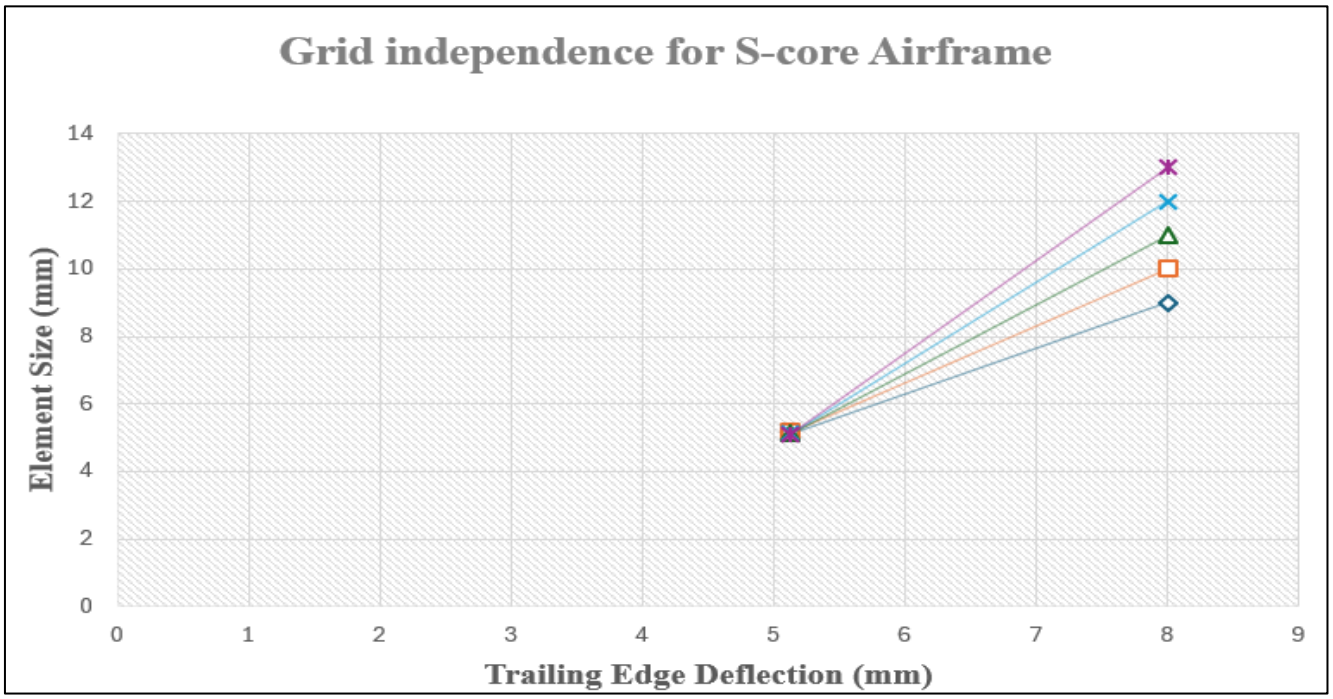

Fig 24: Grid Independence Chart for S-Auxetic

In the following analysis, we have obtained the Equivalent Stress (MPa) and Trailing-Edge Deflection(mm) for the Re-entrant and S-auxetic airframes. The results are plotted for loads ranging from 50-300 N. They're compared to each other by plotting, Load (N) vs Trailing edge deflection (mm) and load(N) vs equivalent stress (MPa) graph from both structures.

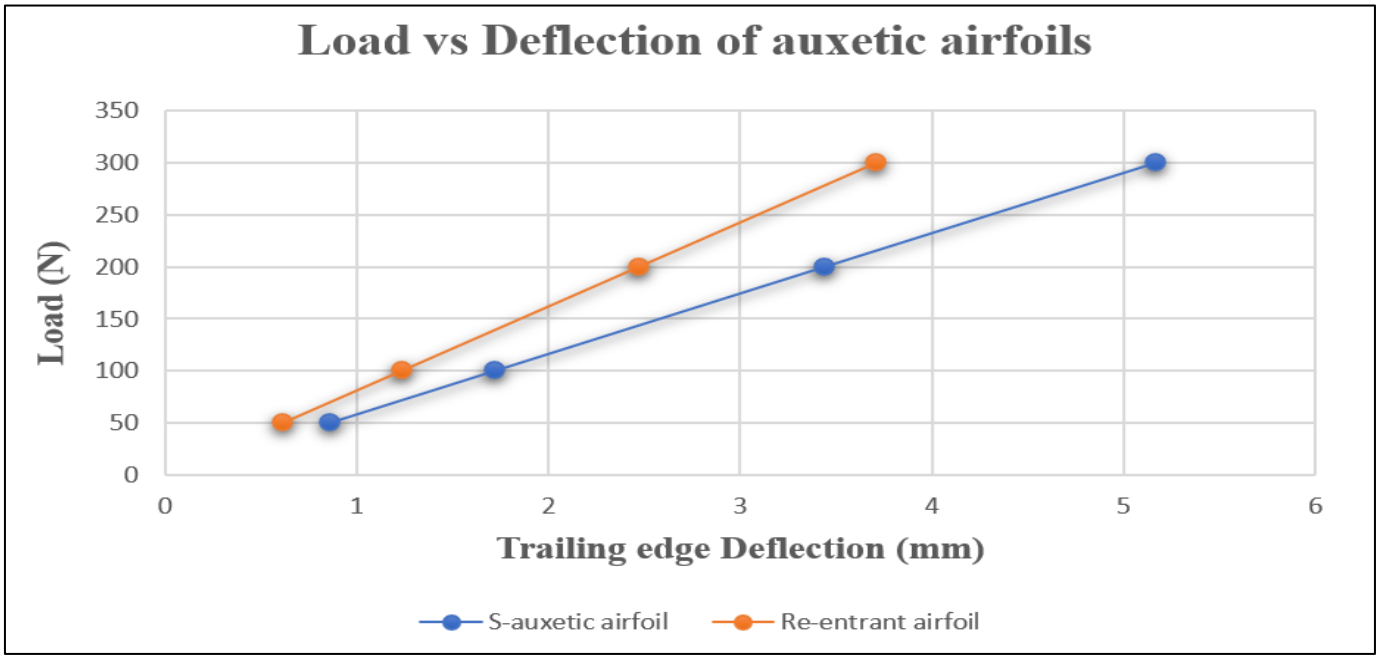

Fig 25: Load vs Deflection

ISSN No:-2456-2165 https://doi.org/10.38124/ijisrt/IJISRT24MAY1201

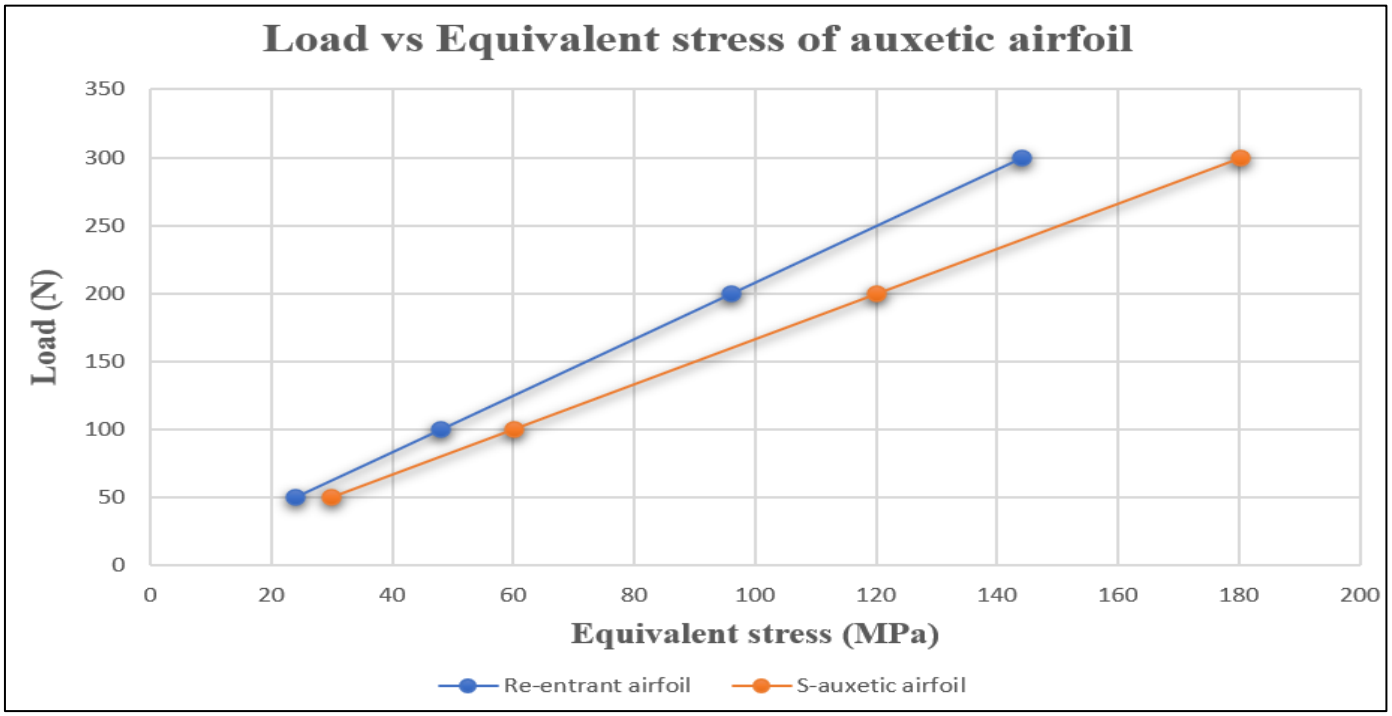

Fig 26: Load vs Equivalent stress

From the above graphs, we can understand that deflection and stress acting on the airframe structure lie under the elastic region. The result obtained for the re-entrant airframe is validated with the reference paper. For the same applied force, the re-entrant auxetic airframe exhibits more flexibility and shows lower stress and deflection when compared to the S-auxetic airframe as shown in Figures 25 and 26.

Through the analysis, the maximum equivalent stress of the Re-Entrant airframe and S-shaped airframe was found to be 143.99MPa and 180.25Mpa respectively. Thus, the Re-entrant airframe exhibits lower stress and hence more flexibility.

ISSN No:-2456-2165 https://doi.org/10.38124/ijisrt/IJISRT24MAY1201

CHAPTER FIVE
MODELLING OF AUXETIC WINGS

The wing's re-entrant and S-auxetic auxetic core were modeled, employing airfoil measurements distinct from those used for validation. However, the wing's dimensions were slightly adjusted, resulting in a wing span of 1 meter as per the reference [1]. Equally spaced, the ribs were strategically positioned throughout the structure. A 1mm-thick skin was meticulously applied to complete the wing, utilizing identical materials as illustrated in the accompanying figure.

The design was made using SOLIDWORKS as shown in the Figure 27 and 28.

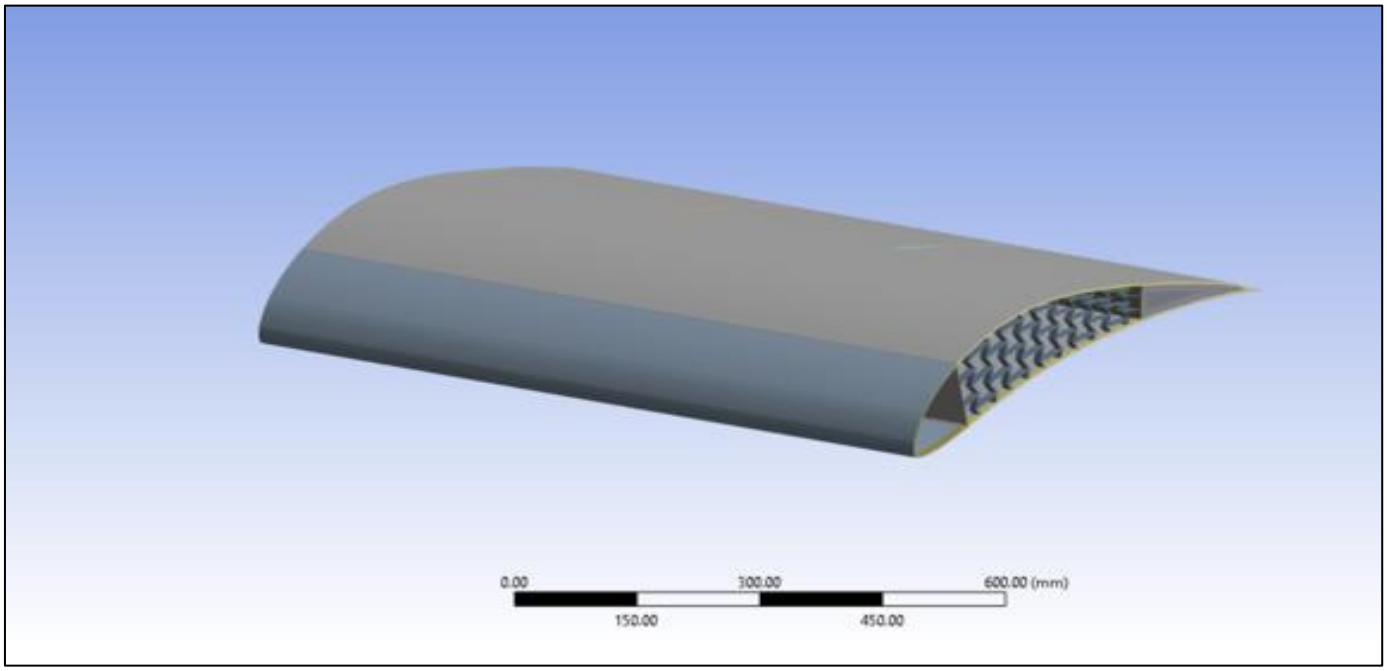

Fig 27: Re-Entrant Auxetic Wing

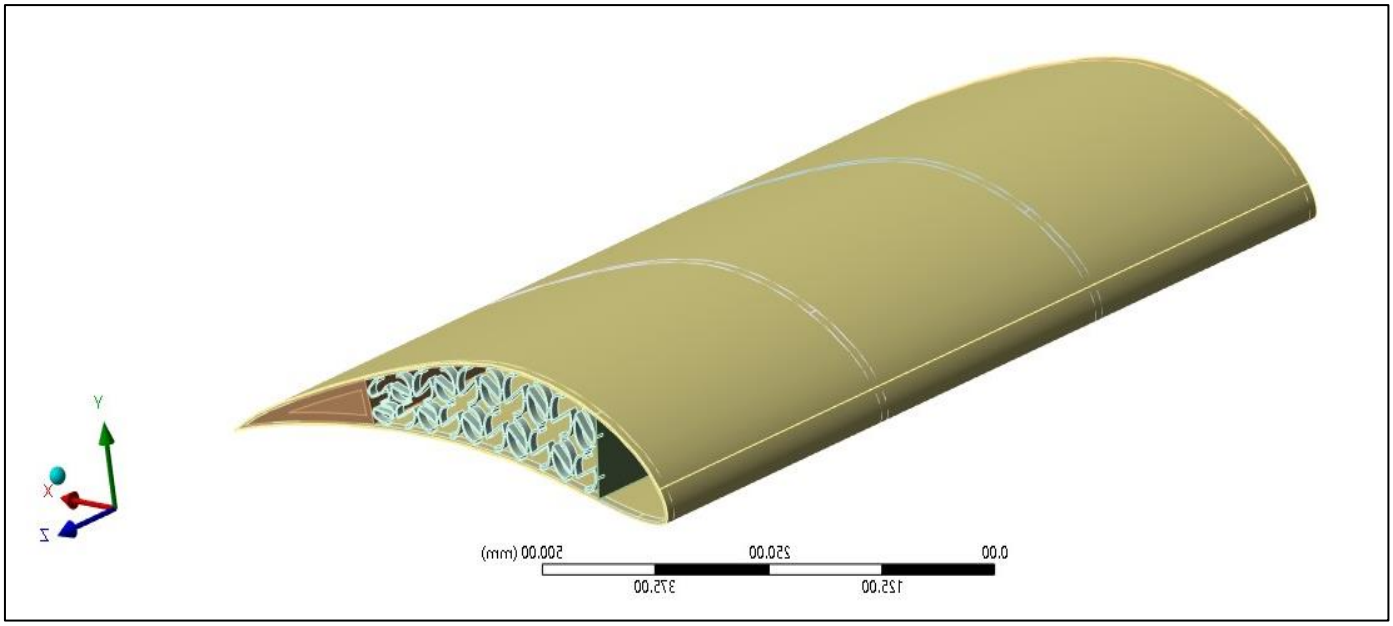

Fig 28: S-Shaped Auxetic Wing

ISSN No:-2456-2165 https://doi.org/10.38124/ijisrt/IJISRT24MAY1201

CHAPTER SIX
COMPUTATION OF AIR LOADS FOR STRUCTURAL ANALYSIS

The wing is assumed to be subjected to a freestream velocity of 154.35 m/s as given in the base paper. The fluid domain is modelled using ANSYS SOFTWARE as seen in Fig 29 and the meshing is done using default mesh. The air-pressure loads that act on the top and bottom surfaces of the airfoils have been studied through fluid dynamic analysis. The dimension of the fluid domain is 10m x 5m x 5m as shown in the figure.

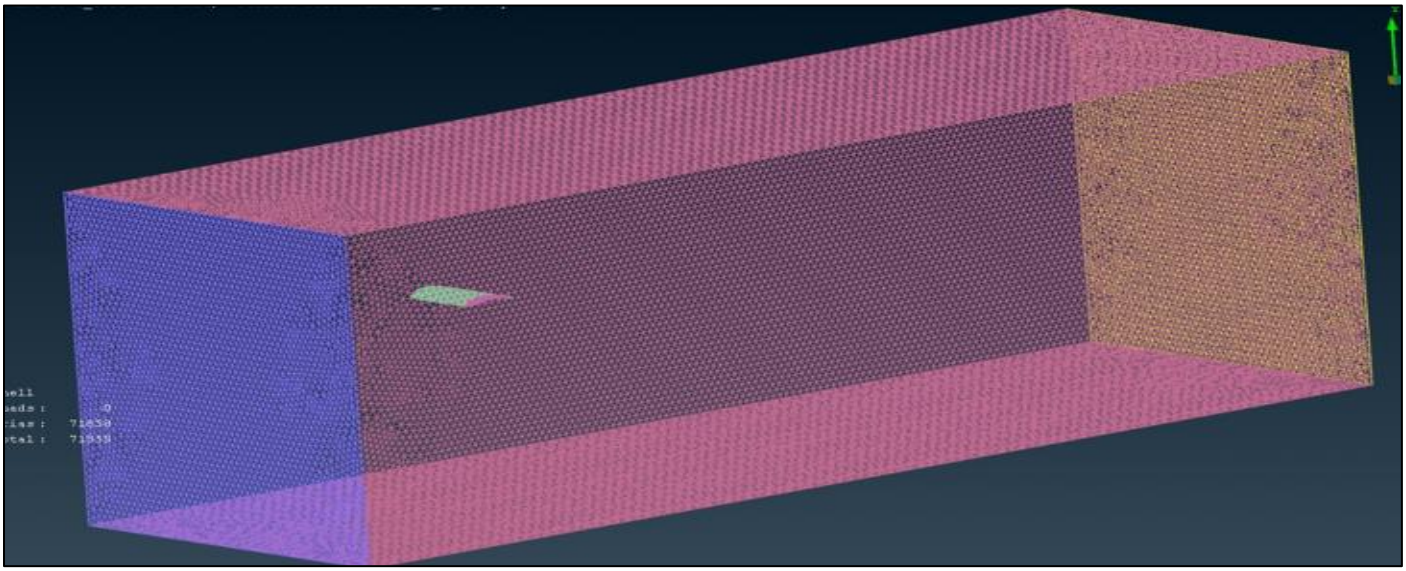

Fig 29: Fluid Domain

The mesh size was given as 500mm and the total number of elements obtained was 1000565. The Standard k-$\mathscr{E}$ model was used to simulate the airflow. The air ideal gas is used as the material and the boundary conditions given are:

- Velocity Inlet: The freestream velocity is 154.35 m/s.
- Pressure Outlet: The Gauge Pressure is given as 0 Pa.
- Symmetry: The face constituting the wing root is given as symmetry.
- Wall: The wing is given as a stationary, no-slip wall.

The monitor points were created for the Coefficient of Lift and Coefficient of Drag. The standard Initialization was given from the inlet and the solution ran for 500 Iterations.

The C_L and C_D were obtained as 0.513 and 0.0654. The lift and drag were obtained as 7201.428N and 916.99N.

The obtained pressure contour results are shown in Figure 30 respectively.

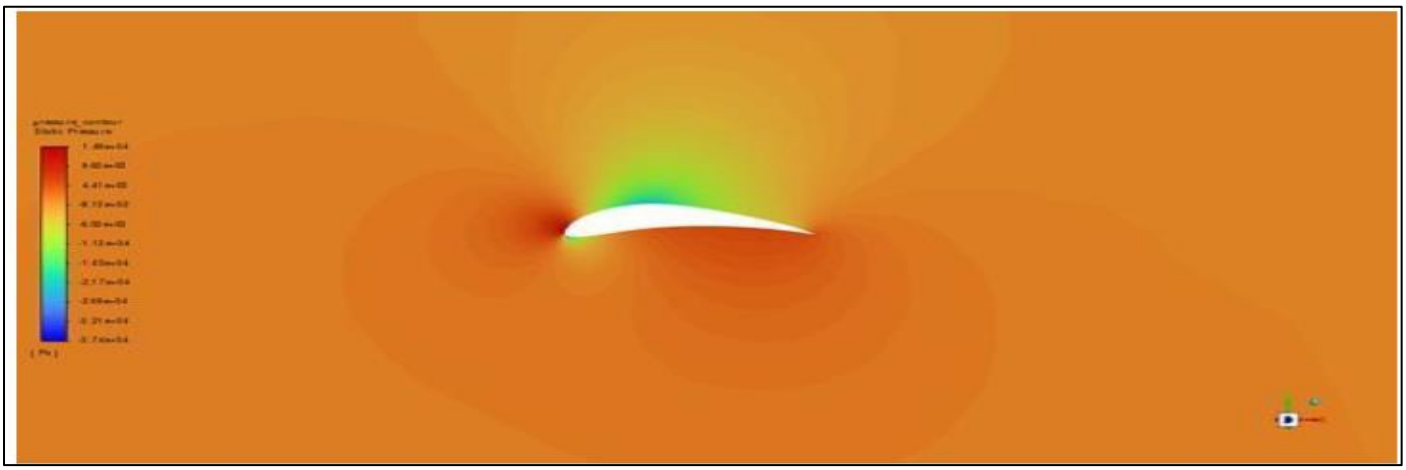

Fig 30: Pressure Contour

ISSN No:-2456-2165 https://doi.org/10.38124/ijisrt/IJISRT24MAY1201

A. Static Structural Analysis of Auxetic Wings

➢ *Re-Entrant Auxetic Wing*

The Static structural setup has been built and the weight of the re-entrant auxetic wing was recorded as 15.62 kg and the total number of mesh elements is 148000.

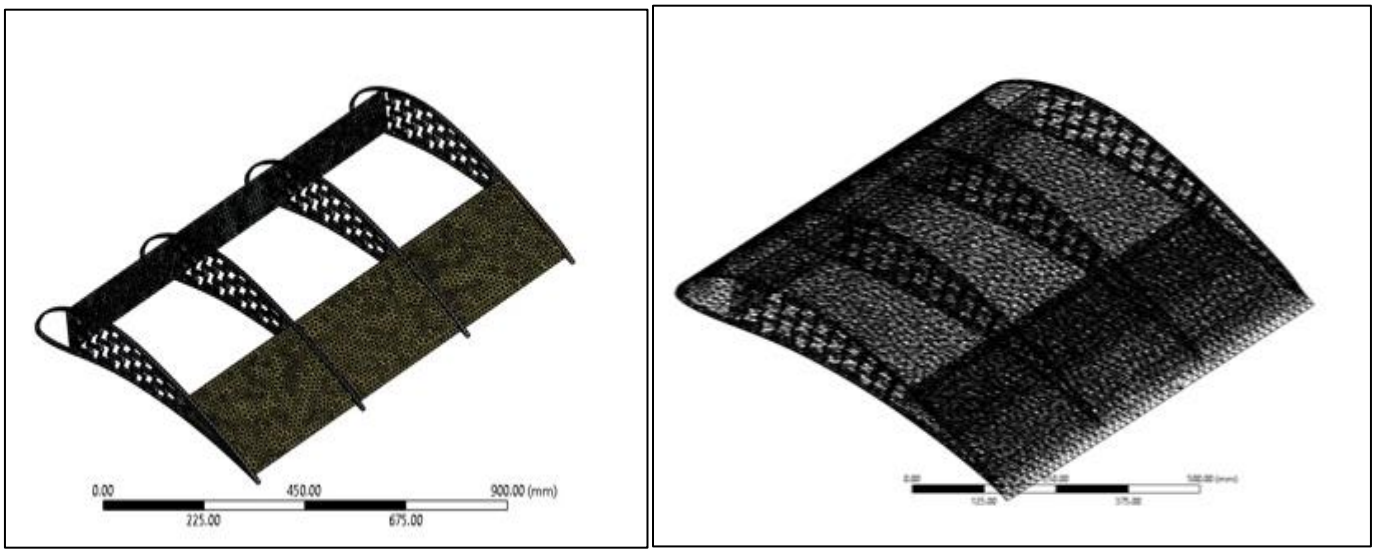

(a) (b)

Fig 31: Mesh of Re-Entrant Auxetic Wing

The wing root was given fixed support and the air-pressure loads were made to act upon the top and bottom surface of the wing as shown in Figure 32. The maximum total deformation with large deflection effects was obtained as 4.564 mm with a maximum equivalent stress of 228.85 MPa. The static-structural results are shown in Fig 33 and 34 and the structure's behavior is observed.

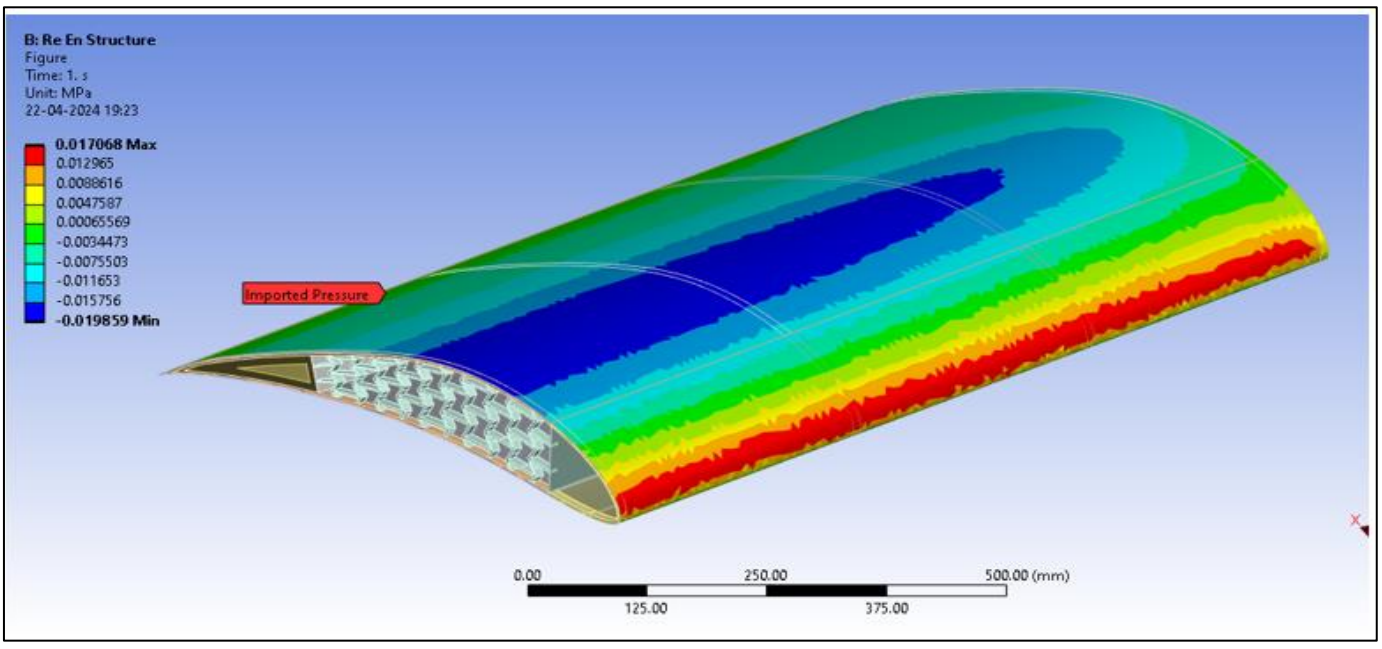

Fig 32: Imported Pressure Loads on Re-Entrant Auxetic Wings

ISSN No:-2456-2165 https://doi.org/10.38124/ijisrt/IJISRT24MAY1201

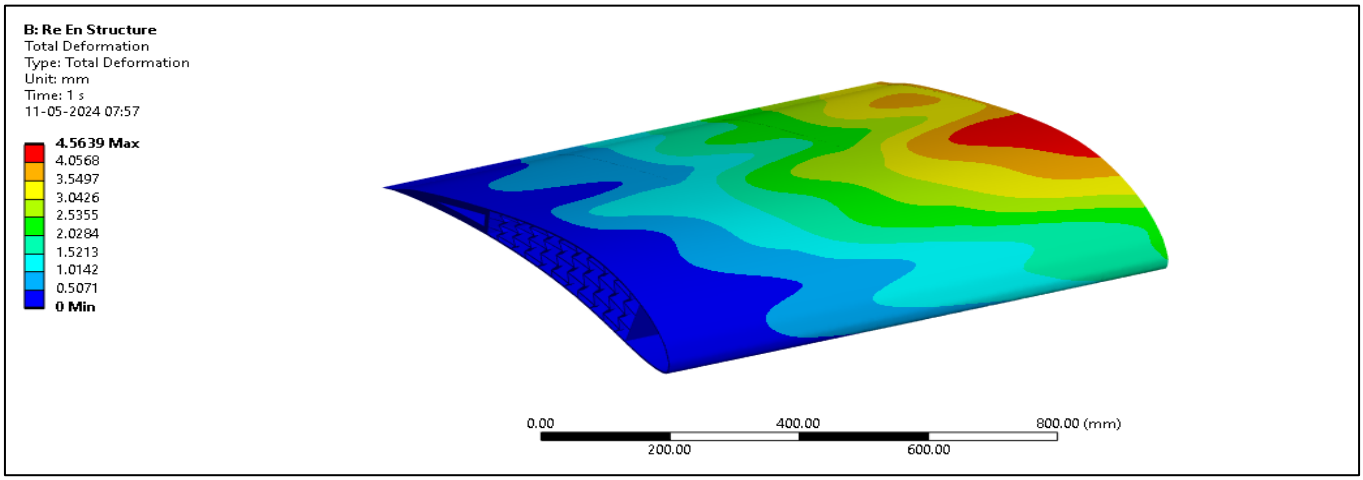

Fig 33: Deformation of Re-Entrant Auxetics Wing

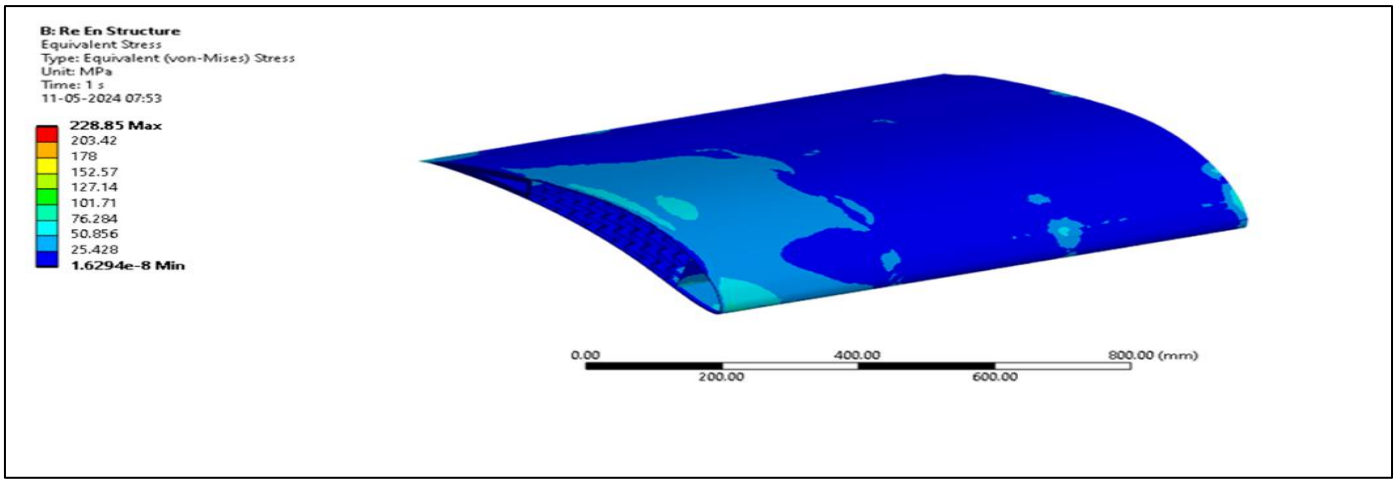

Fig 34: Equivalent Stress Distribution on Re-Entrant Auxetics Wing

➢ *S-Shaped Auxetic Wing*

The Static structural setup has been built and the weight of the re-entrant auxetic wing was recorded as 16.09 kg and the total number of mesh elements is 157000.

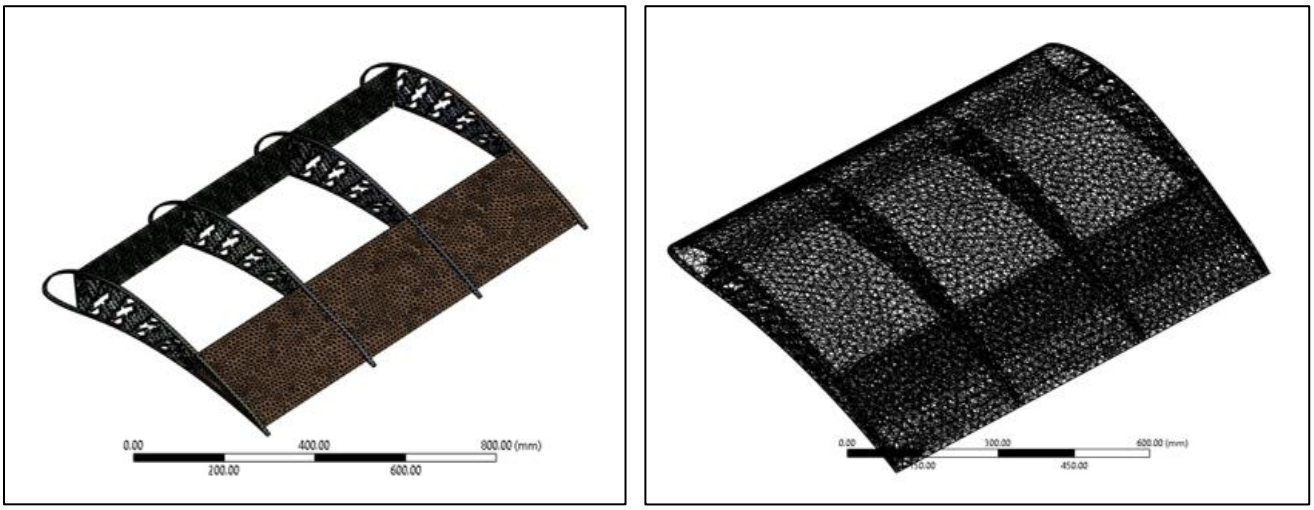

Fig 35: Mesh of S-Shaped Auxetic Wing

The wing root was given fixed support and the air-pressure loads were made to act upon the top and bottom surface of the wing. The total deformation with large deflection effects on was obtained as 5.102 mm with an equivalent stress of 254.25 MPa. The static-structural results are as shown in Fig 7 and 38.

ISSN No:-2456-2165 https://doi.org/10.38124/ijisrt/IJISRT24MAY1201

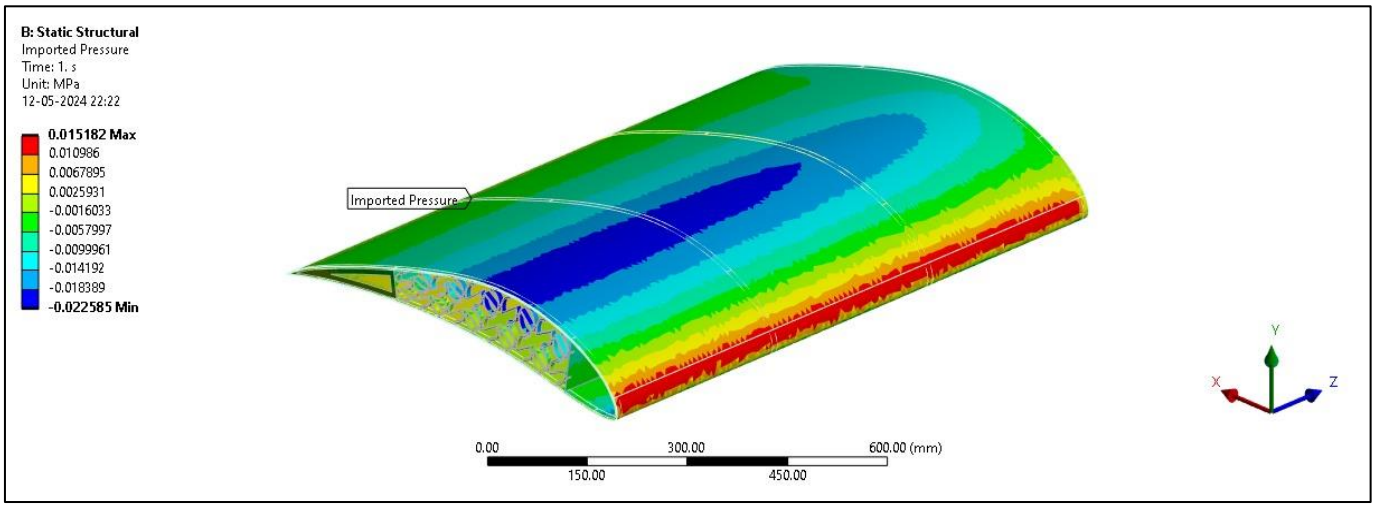

Fig 36: Imported Pressure Loads on S-Shaped Auxetics Wing

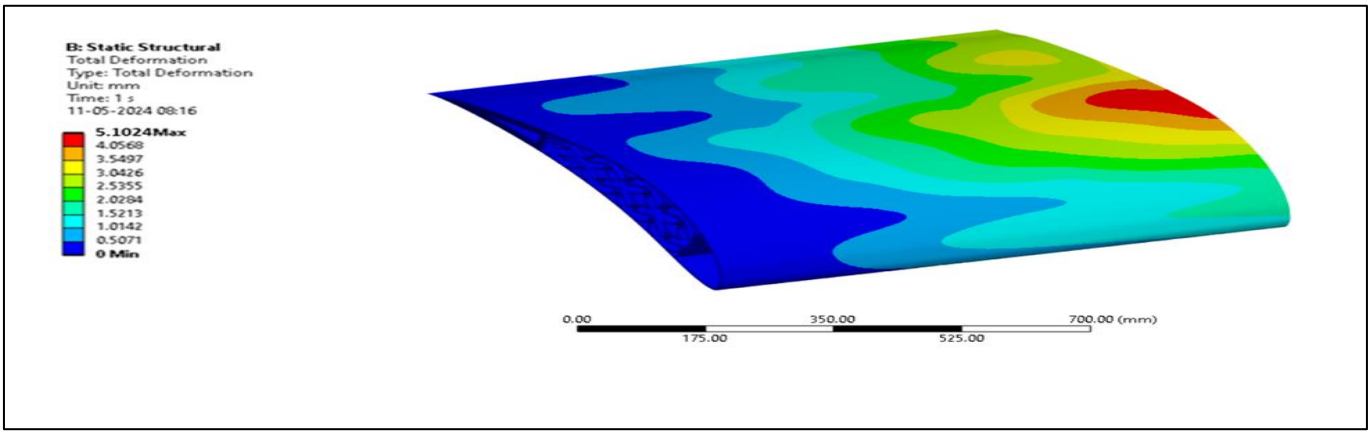

Fig 37: Deformation of S-Shaped Auxetic Wing

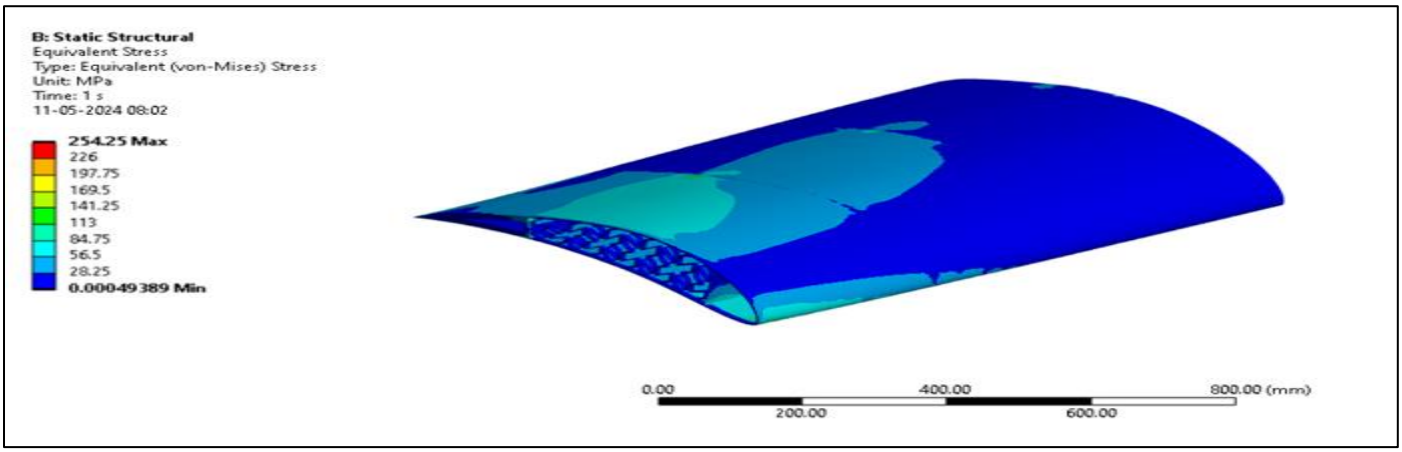

Fig 38: Equivalent Stress Distribution on S-Shaped Auxetic Wing

Based on the results obtained from the above analysis the following observation can be made:

- The stress distribution and deformation obtained for the auxetic wings lie within the elastic region, thus confirming that both structures are within the yield point.
- The static structural analysis shows that the equivalent stress obtained for the re-entrant auxetic wing is 228.85MPa whereas for the S-shaped auxetic wing is 254.25MPa. This shows an **increase of 9.99% in load-carrying capacity** for the Re-entrant auxetic wing, accompanied by a **decrease of 389 grams of weight** when being loaded at the same constraints.

ISSN No:-2456-2165 https://doi.org/10.38124/ijisrt/IJISRT24MAY1201

CHAPTER SEVEN
CONCLUSION

In this paper, we investigated the in-plane mechanical properties of auxetic airframes using re-entrant and S-shaped auxetic patterns and their application in passive morphing for its flexible cores. The morphing airfoil with an auxetic pattern was studied under static structural analysis and aero-static loads.

- The 3D model of the re-entrant Eppler-420 airfoil was designed and validated for static structural and CFD analysis.
- For the same applied force of 300N, the maximum equivalent stress of the Re-Entrant airframe and S-shaped airframe was found to be 143.99MPa and 180.25MPa respectively. With a reduction in stress by 20%, the Re-entrant airframe exhibits lower stress and hence more flexibility.
- Considering the same design parameters and materials, both auxetic wings have also been modelled, taking a span of 1m.
- The CFD analysis was performed by taking inlet velocity as 154m/s as per base paper and C_L and C_D were obtained as 0.153 and 0.061 respectively. And air-loads acting on the wing were captured.
- The fluid-structure interaction was studied on auxetic wings with imported air-loads from CFD on the upper and lower surface of the wing, to observe the structure's behavior and performance.
- It was found that the Re-entrant auxetic wing showed an increase of 9.99% in load-carrying capacity, accompanied by a decrease of 389 grams of weight when compared to the S-shaped auxetic wing. The mass of the re-entrant wing and S-auxetic wing are 15.62Kg and 16.09Kg respectively.

➢ *Future Scope*

- The parametric study can be carried out based on different positions of auxetic patterns.
- To study the aerodynamic properties at different morphing angles.
- The accuracy of air-loads can be further improved by using finer mesh for CFD.
- Weight and structural strength can be improved and enhanced by using composite and other lightweight materials.
- Structural optimization can be carried out to improve the flexibility of the auxetic core.

ISSN No:-2456-2165 https://doi.org/10.38124/ijisrt/IJISRT24MAY1201

REFERENCES

[1]. S. Sivambika, Benitha Shalom, Darsha Reddy K, Vignesh S, Aircraft Wing Morphing using Auxetic structure to control flutter, 2023.
[2]. P R Budarapu, Sudhir Sastry Y B, R NATARAJAN, Design concepts of an aircraft wing: composite and morphing airfoil with auxetic structures, Frontiers of Structural and Civil Engineering. 10 (2016) 394–408, http://dx.doi.org/10.1007/s11709-016-0352-z.
[3]. Hyeonu Heo, Jaehyung Ju, Doo-Man Kim, Compliant cellular structures: Application to a passive morphing airfoil, Elsevier. Comp. str. 106 (2013) 560-569, https://doi.org/10.1016/j.compstruct.2013.07.013.
[4]. Paolo Bettini et.al, Composite chiral structures for morphing airfoils: Numerical analyses and development of a manufacturing process, Elsevier. Comp: Part B 41 (2010) 133-147, https://doi.org/10.1016/j.compositesb.2009.10.005.
[5]. A Alderson and K L Alderson, Auxetic materials, The University of Bolton, UK, https://doi.org/10.1243/09544100JAERO185.
[6]. Avinash Mohan & Prasanna Mondal, Impact Behavior of Auxetic Structures: Experimental and Numerical Analysis", Elsevier. Mater Tod 87 (2023) 292-298, https://doi.org/10.1016/j.matpr.2023.05.631.
[7]. Kusum Meena & Sarat Singamneni, A New Auxetic Structure with Significantly Reduced Stress, Elsevier. Mater & Des 173 (2019) 107779, https://doi.org/10.1016/j.matdes.2019.107779.
[8]. Zeyao Chen & Jianwang Shao, Concepts for Morphing Airfoil Using Novel Auxetic Lattices, ResearchGate. (2020), http://dx.doi.org/10.1007/978-981-15-1773-0_20.
[9]. Krishna Prasath Logakannan, Velmurugan Ramachandran, Jayaganthan Rengaswamy & Dong Ruan, Dynamic Performance of a 3D Re-entrant Structure, Elsevier. Mech of Mater 148 (2020) 103503, https://doi.org/10.1016/j.mechmat.2020.103503.